UiT The Arctic University of Norway

Faculty of Biosciences, Fisheries and Economics, Department of Arctic and Marine Biology

Experimental evidence for species-specific adherence of nanoplastic particles in Arctic phytoplankton communities

Anna Miettinen

Master's thesis in Biology, BIO-3950, November 2022

Experimental evidence for species-specific adherence of nanoplastic particles in Arctic phytoplankton communities

Anna Miettinen

Master of Science in Biology

Supervisors:

Rolf Gradinger – UiT the Arctic University of Norway

Claudia Halsband – Akvaplan-niva

Co-supervisor:

Anna Vader – UNIS the University Center in Svalbard

Abstract

Plastic debris are ubiquitous, and the Arctic is no exception. Despite the relatively low population number around the Arctic, abundances of microplastic litter are like those of the most polluted subtropical areas. Micro- and nanoplastics have been found in Arctic fauna, but due to constraints in methodology, measurements of nanoplastics in sea water have not been carried out yet. Micro- and nanoplastic toxicity tests have recently executed in phytoplankton single species but no literature exists of Arctic taxa, and there is little knowledge how complex communities respond to nanoplastic exposure. To bridge these knowledge gaps, this thesis carried out two experiments, where 1) two sub-Arctic diatoms (*Chaetoceros gelidus* and *Thalassiosira gravida*) were chronically exposed to polystyrene nanoplastics over the course of their exponential and stationary phases, testing for growth and biochemical responses and 2) Arctic phytoplankton communities from the Barents Sea Polar Front were incubated with polystyrene nanoplastics for 3 h. It was assumed that, because some species, such as *C. gelidus* produce high concentrations of sticky transparent exopolymer particles (TEP), that they would have the highest levels of adherence in both experiments. The single species study did not yield any results. Phytoplankton community experiment proved species-specific adherence of nanoplastics, however, contradictory to our hypotheses, presence of TEP may not be the determining factor in adherence. We suggest that, because of the species-specific adherence, there may be a seasonal cycle in adherence related to the seasonality of phytoplankton taxa. These results prove that in the future, natural community experiments must be carried out at an increasing level.

Keywords: nanoplastics, Thalassiosira gravida, Chaetoceros gelidus, Polar Front, adherence

Acknowledgements

First and foremost, I would like to thank my supervisory team Rolf Gradinger, Claudia Halsband and Anna Vader. Thank you for the tireless and patient supervision and expertise on such an interesting topic and taking me under your wing out of the blue. Special note for Rolf, who lit a passion for phytoplankton in me. I came to UiT as a plastics-only interested novice, who quickly turned into someone who talks about algae with a spark in their eyes. Thank you for the expertise, shared passion for the Arctic, giving unforgettable cruise experiences and hours of staring at sea ice, and all your help with carrying this thesis from start to finish.

Thanks to the absolutely best office mates Yasemin, Christine and Martí at NFH, who watched me work in the windowless incubator room like a T-rex. For Karley who saw when I desperately needed coffee and nutrients, for Ulrike who helped with lab expertise.

Finally, to my family and friends, far and close. Thank you for your endless, tireless support, safety network, love and creating a home in a whole new place. And Simen, thank you for your Photoshop and Python skills, and your irreplaceable company.

Abbreviations and nomenclature

AW = Atlantic Water

ArW = Arctic Water

ASW = Artificial sea water

Chl max = Chlorophyll a maximum

CTD = conductivity, temperature and depth instrument

DAPI = 4′,6-diamidino-2-phenylindole

FSW = filtered seawater

MilliQ = ultrapure water

MIZ = Marginal Ice Zone

MNPs = micro- and nanoplastics

NP = nanoplastic

Table of Contents

1. Introduction

1.1. Global plastics: production, pollution and degradation

Plastics production started on a global scale in the 1950s and has grown rapidly to this date, with annual production reaching 380 million tons by 2019 (Bergmann et al., 2022). Plastic as material has a wide range of use, mostly in packaging (Geyer et al., 2017). A huge fraction of plastic waste is mis-managed and only 9 % gets recycled while the rest end up in landfills or get dispersed in the ocean. 4.8-12.7 million tons entered the oceans in 2010 alone (Li et al., 2020). Due to their persistence in the oceans, which has been estimated to be between 100-1300 years depending on the polymer size, color and material (Turner et al., 2020), they can travel long distances from their sources (Elgarahy et al., 2021). The most prevalent polymer types found in the oceans have been polyethylene, polystyrene, polypropylene, polyethylene terephthalate and polyvinylchloride (Elgarahy et al., 2021). Plastic particles in the ocean can be grouped according to size. Small plastic particles can be divided into micro- (>1 µm to ≤5 mm) and nanoplastics (≤1 µm) (Bergmann et al., 2022). Micro- and nanoplastics (MNPs) make up more than 95 % of marine litter and is ubiquitous, including the Arctic (Bergmann et al., 2022; Elgarahy et al., 2021). Microplastics (MPs) can be further divided into primary and secondary MPs. Primary are small virgin pellets which are used a) as raw materials in the industry to make products or b) directly in products, such as cosmetics (Elgarahy et al., 2021). Secondary MPs have fragmented from larger plastics by weathering, UV photodegradation (photo-oxidation), water abrasion, biodegradation, and temperature. When plastic litter end up in the ocean, the degradation of the material is retarded from that of on land because biofouling by organisms starts fast, which in combination of light scattering in water leads to less intense UV-light. Temperature is another factor that determines the activation energy needed for photo-oxidation, thus, as temperature in seawater is lower than on land, it hinders the degradation rate further (Andrady, 2015). Particles lighter than 1 mg get fragmented faster than heavier MPs (ter Halle et al., 2016). In addition to fragmentation, another threat of plastic litter in the oceans emerges from additives and organic pollutants (Elgarahy et al., 2021). Additives are chemicals added to the material during manufacturing to extend their versatility and durability for different uses, including flame retardants, stabilizers, and plasticizers. These chemicals can leach in contact with seawater, and conversely, plastic can ab/adsorb organic pollutants from

the ambient water due to their high affinity, therefore acting as vectors of pollutants for marine biota (Elgarahy et al., 2021).

The Arctic Ocean is no exception when it comes to the widespread occurrence of plastic debris. A recent study found that the Barents Sea plastic pollution with particle sizes larger than 300 μm was equivalent to the most polluted subtropical areas and was the highest for the whole Arctic, with values ranging from 145 to 963×10^3 particles km^{-2} (Cózar et al., 2017; Tošić et al., 2020). It is no surprise, as a mathematical modelling study from 2012 on global surface pollution distribution patterns predicted that within 50 (now 40) years' time, a sixth major surface patch of plastic litter would emerge in the Barents Sea (Sebille et al., 2012). For the ice covered Arctic, an additional important physical force for particle fragmentation may be the sequential freezing and melting cycles and the effects of sea ice (Cózar et al., 2017). The relatively small human population in the coastal areas of the Arctic Ocean compared to the high plastic load is an indication that the Global Thermohaline Circulation (THC) pushes plastic litter to these areas (Cózar et al., 2017). In addition to seawater, plastics have been observed in the sea ice and it can also receive pollution from airborne particles (Kanhai et al., 2020). As sea ice forms, it scavenges particles during nucleation and get incorporated into the sea ice matrix, until particles are released again during melt. This is supported by observations of higher plastic loads in sea ice cores than the seawater beneath with 2×10^3 to 1.7×10^4 m^{-3} and 0-18 particles m^{-3}, respectively (Kanhai et al., 2020). Thus, sea ice can act as a temporal sink for plastics and transport them long distances from the area they were scavenged from (Bergmann et al., 2022).

1.2. Plastic debris in Arctic biota

In Arctic environments, plastics have been found in fish such as polar and Atlantic cod (Kögel et al., 2022), fulmars (Kögel et al., 2022), zooplankton such as amphipods and copepods (Botterell et al., 2022), benthic fauna such as polychaetes (Knutsen et al., 2020) and sea anemones, crabs and starfish (Fang et al., 2021), in beluga whales (Moore et al., 2020) and an unspecified number in other cetaceans and pinnipeds, and the polar bear (Collard & Ask, 2021 and the references therein). These previous findings show that the Arctic is not accumulating

plastics in the environment, but the fauna are in direct and indirect contact with this marine litter.

Because of their size, nanoplastics (NPs) have been studied much less both in the natural environment and in vitro than MPs (Zaki & Aris, 2022). In natural systems, this is mostly due to constraints in the methodology, as standardized procedures have not been implemented yet (Rai et al., 2021). Even though standardized methods for detecting NPs are lacking, first studies are starting to report effects from NPs in organisms exposed to these particles (discussed below). For the natural environment, this constraint still exists and has resulted in the inability to measure plastic debris within phytoplankton communities.

In vitro studies of phytoplankton and MNPs are relatively new as a field, with the first ones reported just a few years ago (Li et al., 2020). Still today, the vast majority of researchers have chosen to expose single species at a time with up to beyond environmental concentrations (Casabianca et al., 2021), but an increasing number are testing environmentally relevant MNP loads as well. The main species used in experiments have been Chaetoceros neogracile, Chlorella vulgaris, Dunaliella tertiolecta, Phaeodactylum tricornutum, Skeletonema sp. and Thalaassiosira sp. (Zaki & Aris, 2022, and references therein). There are a variety of effects recorded of phytoplankton exposed to MNPs, however some seem immune to these particles. Effects were observed on biochemical to physical properties, which could lead to ecologically damaging consequences for phytoplankton. The most common effects observed from exposure to MNPs in phytoplankton have been growth inhibition and oxidative stress (ROS) (for example: Fulfer & Menden-Deuer, 2021; Wang et al., 2021; Wu et al., 2021; Zhang et al., 2021), and some less frequent ones include decrease in chlorophyll content and photosynthetic efficiency (for example: González-Fernández et al., 2019), cell membrane damages (for example: Mao et al., 2018), exogenous stress and even apoptosis (Su et al., 2020). Some of these adverse effects have only been temporary. Observations are not conclusive, as some species have not been affected at all (Baudrimont et al., 2020), and sometimes even higher chlorophyll content has been recorded (Su et al., 2020).

1.3. Barents Sea Polar Front oceanography and biology

There are no previous studies of the occurrence of MPs in the Barents Sea Polar Front region. It is a boundary structure which divides the relatively warm and saline Atlantic Water (AW) in the south, and cold, fresh Arctic Water (ArW) in the north (Pfirman et al., 1994). This front divides the Barents Sea approximately in half, and its location is relatively stable driven by the bottom topography and ocean currents (Gawarkiewicz & Plueddemann, 1995). AW at the front derives from the Norwegian Atlantic Current, whereas ArW is formed during fall and winter by convection through sea ice formation (Pfirman et al., 1994). Therefore, NPs can be found of both Arctic and North Atlantic origin in this area. Primary productivity varies in this area (Reigstad et al., 2011), and it may be enhanced some years (Børsheim et al., 2014). However, phytoplankton blooms support the Barents Sea food web, feeding zooplankton, mainly Calanus (Falk-Petersen et al., 2009, p.), which are eaten by fish, such as capelin (Basedow et al., 2014). The capelin is a key food species for Atlantic and Polar cod, seabirds, seals and whales (Sakshaug, 1991) and also a commercially important species (Gjøsæter, 1995). This area serves as an important feeding area for predators, such as cod, harp seal and minke whale (Bogstad et al., 2015). Ultimately, Polar Front is an important area for biota and can be called a hotspot in this area.

Prevalent groups of phytoplankton taxa in the Polar Front during peak bloom include diatoms such as Chaetoceros gelidus (previously noted as C. socialis in the Arctic; Chamnansinp et al., 2013), Thalassiosira antarctica var. borealis, and the haptophyte Phaeocystis pouchetii (Rat'kova & Wassmann, 2002). Other, less abundant but noteworthy groups are dinoflagellates like small Gymnodinium spp., ciliates like Tintinnida and other small "naked" flagellates (Wassmann et al., 1999). Pennate diatoms (Pennales) usually start the bloom and get replaced by centric diatoms (Centrales) (C. von Quillfeldt, 1996). Many phytoplankton produce sticky extracellular mucilage, which may be found surrounding the cell or as free particles in the ambient water (Passow, 2002b). Transparent exopolymer particles (TEP) are a subcategory of exopolymeric substances (EPS) as they are discrete, Alcian blue -stainable particles. They consist of polysaccharides (Thornton, 2002) and are a major component of marine snow, which is the main element of vertical flux of carbon, and serves as a source of food for larger zooplankton (Passow, 2002a). Two major producers of TEP during phytoplankton blooms in the Arctic are Chaetoceros gelidus and Phaeocystis pouchetii. For P. pouchetii, this mucilage acts as a substrate to form colonies (Throndsen, 1997), and acts as a substrate for phytoplankton aggregation. TEP concentrations can get especially high in the post-bloom stage when

environmental conditions have deteriorated and under stress (Thornton, 2002), but they can also get high when cells are healthy (Penna et al., 1999).

1.4. Aims of the thesis

Two experiments were conducted in this thesis. First, to attempt to bridge the knowledge gap of how NPs interact in a mixed phytoplankton community, we exposed phytoplankton communities from the Arctic to virgin polystyrene nanoparticles in a short-term experiment. To our knowledge, there is no existing literature of similar studies. We argue that studying the response of a complex phytoplankton community on nanoplastic exposure is urgently needed, as the interactions and encounters with NPs and microalgae may differ from that of single species modelling experiments (Casabianca et al., 2021). Concentration of TEP will serve as proxy for stickiness in the population. Second, to assess whether a chronic exposure to polystyrene nanoplastics will have biochemical or growth effects on sub-Arctic diatoms, Thalassiosira gravida and Chaetoceros gelidus were chosen for a longer study. This contributes to a better understanding of how these diatoms react through their exponential and stationary growth phases, and whether they are able to counteract the effects. T. gravida is a cosmopolitan species (Halse & Syvertsen, 1996), whereas C. gelidus is present in the Northern hemisphere (Chamnansinp et al., 2013). TEP will serve as a proxy for stickiness potential, and as a stress response.

The overarching goal of this thesis was to study the potential for interaction between sub-Arctic and Arctic microalgae and nanoplastic particles, mainly the adherence of particles to microalgal cells. The main objectives were

1) Determining the degree and type of adherence of NPs on microalgal cells in both algal monocultures and mixed communities.
2) Observing possible differences between level of adherence between protist groups in the mixed community, and differences are linked to the number of species specific TEP production.
3) Assessing biochemical responses to interactions with NPs, specifically in diatom monocultures.

We hypothesize, that

A) Polystyrene nanoplastic particles adhere to microalgal cells.
B) Protists in the phytoplankton community will differentiate in levels of adherence which is related to the presence of TEP within the community. The highest TEP producing phytoplankton have the highest rates of adherence compared to their relative abundance.
C) Chaetoceros gelidus show adverse biochemical effects, such as lower Chlorophyll a (Chl a) concentration, decreased efficiency of photosystem II (PSII), increased production of TEP as a stress response and hindered growth during exponential phase. The effects are reversible, and C. Chaetoceros recovers during stationary phase. Thalassiosira gravida will have little to no effects due to lower production of TEP.

2. Materials and Methods

In this study, two separate experiments were conducted, where the main goal was to determine the adhesion of NPs to microalgae. More specifically, in the first experiment, sub-Arctic diatom monocultures were exposed to two different particle concentrations of a nanoplastic and a non-plastic reference particle for longer periods in controlled experiments, to study the adhesion of particles to algae and algal growth responses resulting from this interaction. In the second experiment, Arctic mixed microalgal communities were exposed to NPs on short time scales, to study the selective adherence of NPs to different taxonomic groups.

2.1. Experimental study with monocultures

Cultures of two colony forming diatoms species, Chaetoceros gelidus and Thalassiosira gravida were exposed to two kinds of nanoparticles over the course of their exponential and stationary growth phases. While polystyrene NPs were the particle of main interest, silica nanoparticles were used as non-plastic reference particles to see if non-plastic particles yield similar effects to plastics.

2.1.1. Algal cultures, particles and reagents

Algal stock monocultures (originating from the Barents Sea) of Thalassiosira gravida and Chaetoceros gelidus were obtained from Bente Edvardsen, University in Oslo. These species were selected as they are both centric diatoms but differ in the amount of produced TEP. Cultures were exposed to two different particles: polystyrene (PS) and silica (Si) particles, both 1.0 µm. The plastic particles used were blue-green fluorescent 430/465 nm (excitation/emission) polystyrene particles (NPs) (Thermo Fisher Scientific Inc., USA). The silica beads (Kisker Biotech GmbH & Co. KG, Germany) had an excitation/emission rate of 354/450 nm, respectively.

The original particle suspensions were diluted by pipetting 5.0 µL of the purchased polystyrene solution ($1x10^{10}$ particles L^{-1}) into 50 mL artificial sea water (ASW) in a Falcon tube. In the next step 2.5 mL of this work solution (10^6 particles L^{-1}) was pipetted into treatment bottles

filled with algal cultures (250ml, Nalgene®, Thermo Fisher Scientific Inc, USA) to reach a final nominal concentration of $1x10^4$ particles L^{-1}. Similarly, the silica particle solution was diluted by pipetting 10.4 µL ($4.8x10^{10}$ particles L^{-1}) to 50 mL ASW in a Falcon tube. In the second step, 250 µL ($1x10^7$ particles L^{-1}) of working solution was pipetted into the algal filled treatment bottles to reach a similar final concentration as for polystyrene particles.

2.1.2. Algal culture medium and growth conditions

ASW was produced and used as a growth base (for chemical composition, see Appendix A). It was filtered through 0.45µm filter (VacuCap®, Pall Laboratory), sterilized in an autoclave and salinity adjusted with sterilized MilliQ water to reach final salinities between 32-33psu. For the algal growth experiment, Guillard's growth medium was added to reach f/2 concentration.

The received initial algal stocks were upscaled (i.e., cell concentration was increased) from stock cultures by adding 7.5 mL stock culture into 142.5 mL ASW to reach sufficient cell concentrations for the experiment. They were kept in an incubator at approximately +3.3 °C with 24h irradiance at 175.2 µmol photons m^{-2} s^{-1}, until the cell concentration reached $1x10^6$ cells L^{-1} for C. gelidus, and $5x10^5$ cells L^{-1} for T. gravida.

2.1.3. Experimental design

Two experiments were done with roller tanks between Dec 10^{th}-21^{st}, 2021 and Mar 12^{th}-25^{th}, 2022, with C. gelidus and T. gravida, respectively. Algal cultures were exposed to NPs at constant irradiance (160.1 µmol photons m^{-2} s^{-1}) and temperatures of +2 °C and +4 °C for T. gravida and C. gelidus, respectively, with rolling speed of 2.91 rpm. The experiment for each species contained five different treatments: control, and PS and Si particle additions in low and high concentrations, respectively (Table 2). Each treatment was triplicated, in addition to five initial control ("extra") bottles for day 0. The purposed of these extra bottles was to be used as initials and thereby conserve volumes in the main treatment bottles, as by the end of the experiment, the volume in treatment bottles was not supposed to go below 50 % of the original. Sampling was done three times during the experiment: day 0, once during exponential growth phase and another time during stationary phase. The two latter sampling times were determined based on growth curve for each taxa, which were established during the experiment (Figure 1).

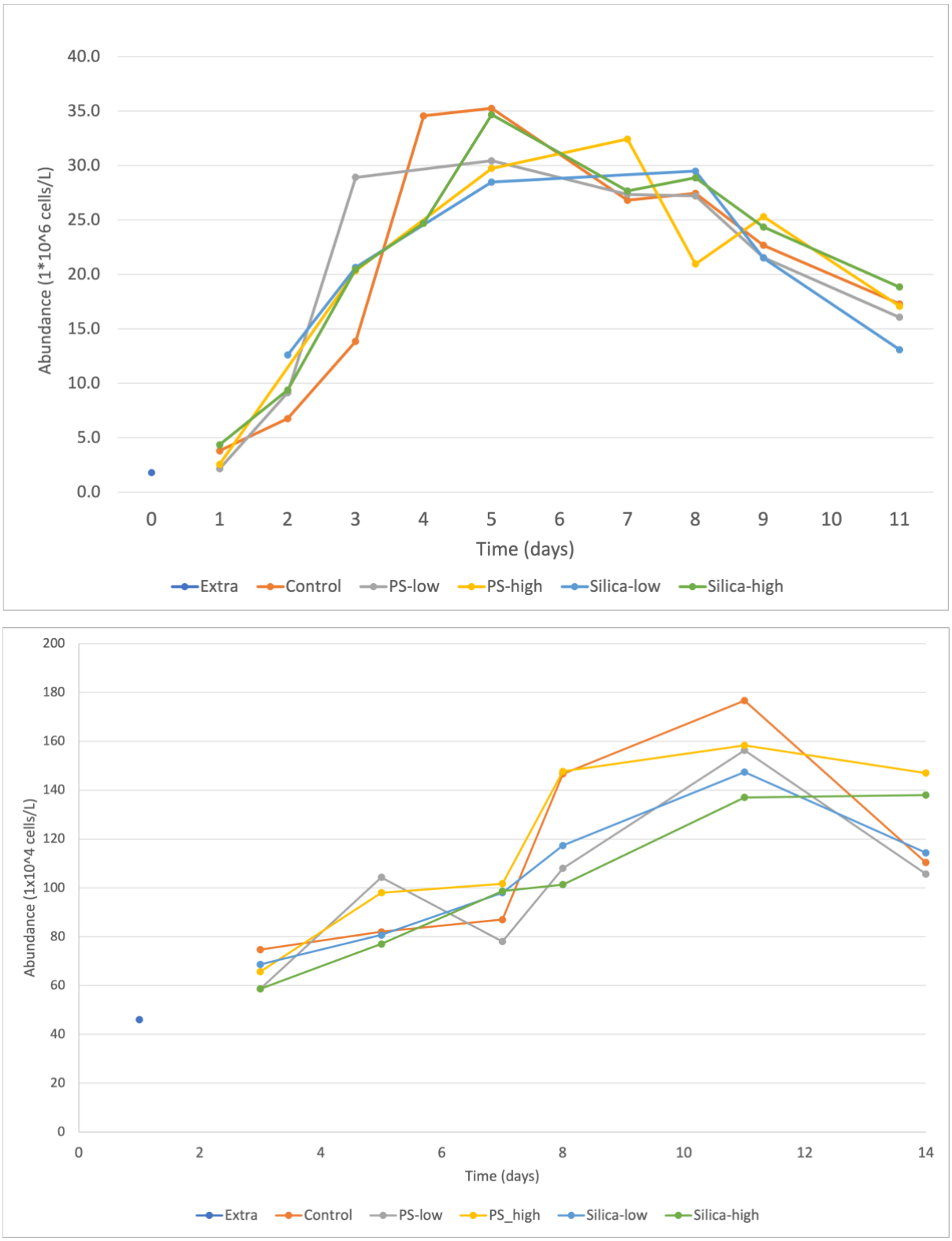

Figure 1: Experimental growth curve of a) Chaetoceros gelidus and b) Thalassiosira gravida.

Table 1: Treatment design for the two monoculture experiments: list of treatments and their replicates for each species.

Species	Treatment	Treatment name	Replicates
T. gravida	No particles	Control	3
T. gravida	No particles	Initial t_o control ("extra")	5
T. gravida	Polystyrene 500 mL^{-1}	PS Low	3
T. gravida	Polystyrene 10 000 mL -1	PS High	3
T. gravida	Silica particles 500 mL^{-1}	Si Low	3
T. gravida	Silica particles 10 000 mL^{-1}	Si High	3
C. gelidus	No particles	Control	3
C. gelidus	No particles	Initial t_o control ("extra")	5
C. gelidus	Polystyrene 500 mL^{-1}	PS Low	3
C. gelidus	Polystyrene 10 000 mL^{-1}	PS High	3
C. gelidus	Silica particles 500 mL^{-1}	Si Low	3
C. gelidus	Silica particles 10 000 mL^{-1}	Si High	3

Prior to the experiment, treatment bottles were first randomized and then anonymized with a secondary labeling system. The algal work cultures (450 mL) were added to a large container with 4550 mL ASW and 18.2 mL of Guillard's growth medium at f/10 concentration. The container was gently rolled on the table to mix algae with growth medium, and 250 mL of algal suspension was distributed to each of the treatment bottles. All treatment bottles except for extras were placed on a roller table in their numeric order (Figure 2), the extra bottles were placed onto the side of the roller table to stand on top of the LED lights.

Table 2: Sampling times for C. gelidus (marked with X) and T. gravida (marked with Y) for all variables. For C. gelidus, sampling for different treatment bottles was done every second day, however not all treatments were checked the same day, thus table shows daily counts. For explanation of variables see text.

Day no.	Cell counts	TEP	Chl a	DAPi	Fv/Fm	Inorg. Nuts.
0	XY	X	X	X	X	X
1	X					
2	XY					

3	X					
4	XY	Y	Y	Y	Y	
5	X					
6	Y					
7	X	XY	XY	XY	XY	Y
8	X					
9	X					
10	Y					
11	X	X	X	X	X	X
12						
13	Y					

Figure 2: Roller table setup for monoculture experiments. Treatment bottles were placed inside the roller tank (five in each), used for slow mixing of the bottles.

2.1.4. Sampling parameters during the monoculture adherence experiment

2.1.4.1. Determination of algal growth curves

Growth rates were calculated based on determination of abundances approximately every second day of the experiment. Cell counts were performed using a Jessen counting chamber (Assistent R; 0.400 mm x 0.0625 mm^2). Subsamples with a volume of 28 µL each were pipetted from each treatment replicate into the counting chamber. Depending on the cell density, cells from areas of 5-25 grids were counted under a stereomicroscope. Growth curves for each species were constructed based on the cell counts by adjusting the counting area of the chamber for each count, and then calculating cells per liter as an average for each treatment.

2.1.4.2. Chlorophyll a fluorescence

Chl a concentrations were measured to evaluate the growth of the diatom cultures. Samples for Chl a (20ml) and TEP analyses (25ml, see below) were taken from the same 45ml subsample, and placed into a Falcon tube each. Chl a samples were filtered using Whatman GF/F filters (0.7 µm) and rinsed with MilliQ water. Then, each filter was placed inside a glass vial, and 10

mL of 90 % acetone was added. The glass vials were placed in a dark refrigerator overnight. The following day, Chl a fluorescence was measured with a Turner Trilogy Fluorometer following the acidification approach (Arar & Collins, 1997)

2.1.4.3. Transparent exopolymer particles

TEP determination is a measure of the concentration of >0.4 µm polysaccharide particles in the sample, which was used as an indication for stickiness in the cultures and a stress response for exposure to particles. TEP samples were filtered onto 0.4 µm PC filters, with Whatman GF/F filter as support underneath. Then, filters were folded and put in cryovials and frozen at -20 °C for further analyses. The concentration of TEP in these samples was determined by a modified method from Arruda Fatibello et al. (2004) by Ulrike Dietrich.

2.1.4.4. DAPI staining

DAPI is a DNA specific fluorescent stain which binds to the nuclei of organisms. It was used to make the diatom cells visible under a fluorescent microscope, allowing to inspect the diatoms in parallel with fluorescent polystyrene and silica particles. Staining was done according to Porter & Feig (1980). Briefly, in centrifuge tubes, a 10 mL subsample from each treatment was fixed with hexamethylenetetramine buffered formaldehyde at 1 % concentration. Then, samples were stained with 10 µL DAPI stain for 10 minutes, and then filtered onto a 0.2 µm PC filter. The filter was preserved on a microscope slide with immersion oil and cover glass, and frozen at -20 °C for microscopic inspection of particle adherence to cells.

2.2. Experimental study with Arctic phytoplankton communities

2.2.1. Study area

The study was conducted along a north to south transect across the Barents Sea Polar Front onboard R/V Helmer Hanssen between 17th and 20th of May 2021 (Figure 3). Study transect was conducted from north to south, where Station 1 was the northernmost and Station 6 southernmost (Figure 1). The five northernmost stations were close together covering the

gradient across the front, whereas Station 6 was located further south in the core of the AW inflow. Sea ice cover during the expedition extended south of the Polar Front to approximately 77.00 N and was located between Stations 2 and 3. Sea ice was present until Station 3, and the last two sampled stations were in open water. Station 5 was not sampled due to poor weather.

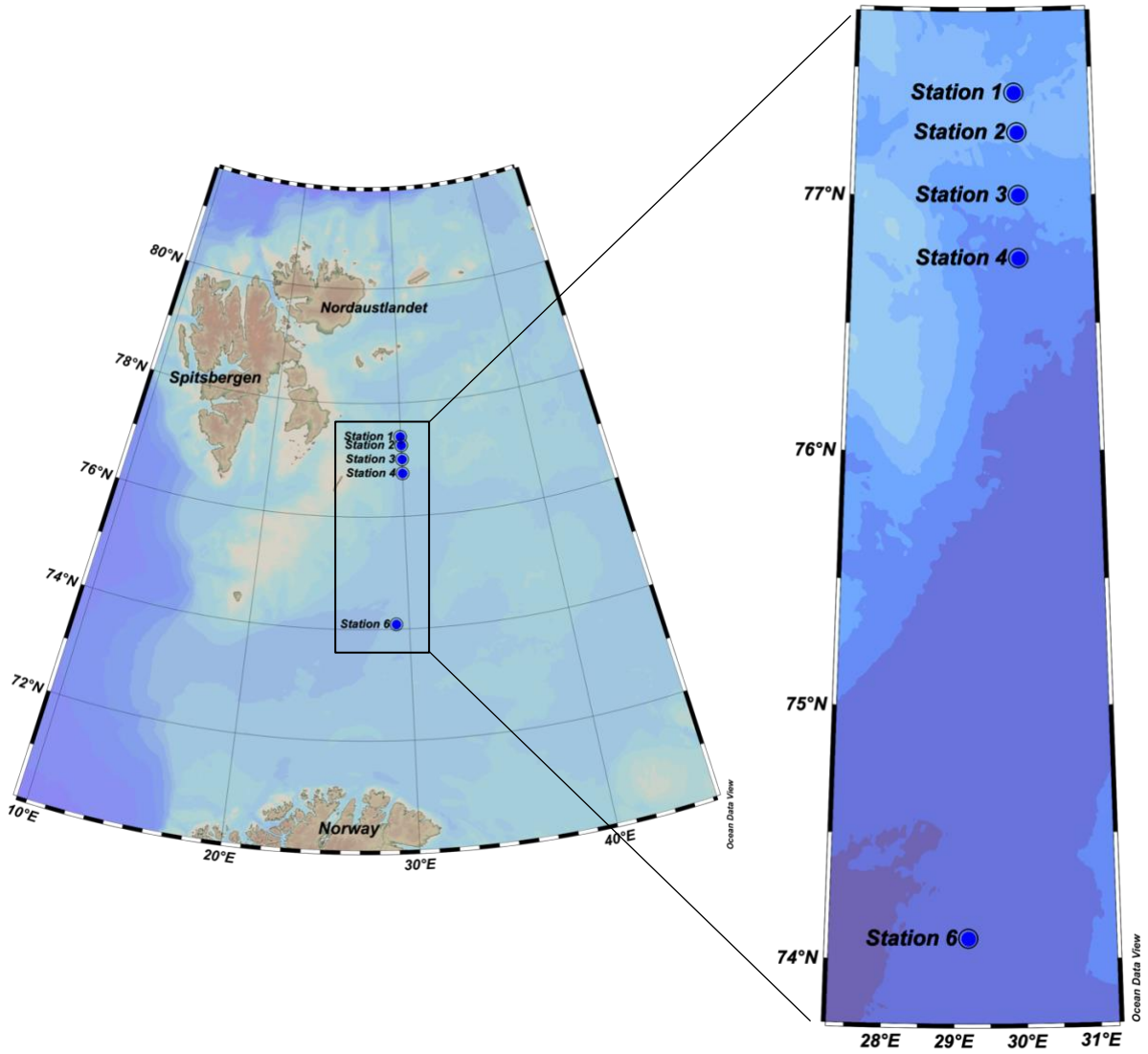

Figure 3. Study area and sampling stations across the Polar Front in the Barents Sea.

Table 3. Environmental conditions of sampling stations (information from the ship's log system Scanmar CGM, various sensors).

Station	Latitude (decimal degree)	Longitude (decimal degree)	Time (UTC) hh:mm	Date (2021)	Depth (m)	Chl max depth (m)	Air temp (°C)	Surface water temp (°C)
S1	77.24 °N	29.57 °E	07:41	May 17th	201	15	-4.6	-1.4
S2	77.14 °N	30.00 °E	12:56	May 17th	194	25	-4.9	-1.5
S3	77.00 °N	30.01 °E	12:26	May 18th	238	20	-3.7	-1.1
S4	76.45 °N	30.00 °E	05:13	May 18th	257	25	-3.1	-0.2
S6	74.05 °N	29.11 °E	08:22	May 20th	358	30	+0.2	+3.9

2.2.2. Field collection of phytoplankton communities

Samples for this study were collected at five of the six stations (Station 5 not sampled) over the course of three days (Table 3). Water samples were retrieved using 8 L Niskin bottles attached to a CTD Rosette at the depths of the Chlorophyll a maximum (Chl max; overall mean 23.2 ± 5.3 m). The Chl max depth was determined at each station by first lowering the CTD Rosette to the sea bottom while simultaneously measuring chlorophyll a specific in situ fluorescence. The CTD Rosette was stopped for approximately one minute at each sampling depth to make sure the open Niskin bottles were completely flushed with water from the desired depth. After the CTD Rosette was on deck, water samples were taken out into carboys and stored in a cool (approximately +4 °C) and dark place until further processing. Water samples were taken from a single Niskin bottle at each station.

2.2.3. NP adhesion experiment with phytoplankton community

The experimental setup included three replicate samples (200 mL) of natural phytoplankton communities from the Chl max depth incubated together with fluorescent 1.0 µm polystyrene particles (Thermo Fisher Scientific Inc., USA). Three replicate cell culture flasks were filled with 200 mL replicate samples and fluorescent NPs were pipetted from the working solution (see Section 2.1.1.) into each treatment bottle at a final nominal concentration of 10 000 particles $mL^{-1,}$ (equivalent to $5.52x10^{-9}$ mg L^{-1}). The treatments were covered and placed in a cold room (approximately +4 °C) and complete darkness for three hours. During this exposure time, the flasks were mixed gently by inversion three times once every hour to prevent sinking of the algae and NPs and ensure opportunities for interactions between algae cells and NP particles.

Experiments were terminated by preserving the flask contents with hexamethylenetetramine buffered formaldehyde at 1 % final concentration. A subsample of 10-30 mL from each preserved sample was stained with 10 µL of an epifluorescent dye (DAPI, 0.1 mg mL^{-1}, excitation 405 nm, Porter and Feig 1980) for approximately 10 minutes and then filtered onto a 0.2 µm PC filter. After rinsing with filtered seawater (FSW) the filter was placed onto a microscopy slide, covered with immersion oil and a microscope cover slip, and stored frozen at -20 °C in darkness for later microscopy analyses.

2.2.4. Phytoplankton identification and characterization

The DAPI stained phytoplankton and other protists were identified and enumerated at 20x and 40x magnifications using a fluorescence microscope (Leica Biosystems). The microscope had two different filter sets for a) blue light excitation for chlorophyll fluorescence to identify photo- and mixotrophic protists and b) UV excitation for DAPI fluorescence and both photo-, mixo- and heterotrophic protists. Species/taxa identification was based on training received from three specialists (Rolf Gradinger, Cecilie von Quillfeldt and Philipp Assmy), and identification keys/books (Halse & Syvertsen, 1996; Lynn, 2009; Steidinger & Jangen, 1997; Throndsen, 1997). For centric diatoms, two groups were identified to genus level (Thalassiosira spp. and Chaetoceros spp.) as well as a taxon of haptophytes belonging to the genus Phaeocystis. Other phytoplankton taxa were grouped into: pennate and other centric diatoms, phototrophic dinoflagellates, heterotrophic dinoflagellates, mixotrophic ciliates, heterotrophic ciliates, phototrophic flagellates, and heterotrophic flagellates. The added

polystyrene particle fluorescence was also visible with 430/465 nm (excitation/emission), and DAPI stain was excited at 405 nm. The limitation to fluorescent illumination of the filtered samples limited the identification, as certain cell and colony morphological features were not visible and identification had to rely on other features, such as size, number and appearance of nuclei, chloroplasts, and the general shape of the frustule. In some cases, both external and internal properties were more visible, like in ciliates and dinoflagellates. Differentiation between Thalassiosira spp. and Chaetoceros spp. was usually based on cell size, as the former can be up to 40 µm in diameter, while most Chaetoceros spp. are only half this size. However, when the features were not distinct enough to determine the genus of centric diatoms, the cells were recorded as part of the category 'other centric diatoms'. For dinoflagellates, the clear and large sized nuclei in addition to the carved shape of the exterior polysaccharide plates were good indicators. Their size range is highly variable, from 20 µm to several hundreds of micrometers. Ciliates were identified based on their nuclear dualism (macro- and micronucleus) in addition to their cilia and – for tintinnids – presence of a lorica on top of their large size (typically 100 µm). "Naked" flagellates are a highly diverse group but often very small (2-20 µm), so they were mostly identified based on their size and asymmetrical shape. Phaeocystis (pouchetii) is very distinct from other flagellates, as their autofluorescent chloroplasts displayed kidney-like shapes, and they size was around 4-8 µm. In general, colonies were recorded when two or more cells were observed clearly in a colony form.

2.2.5. Determination of adherence to individual species

Adherence was determined with the abovementioned microscope samples. The abovementioned protist categories occurred in sufficient abundances and were possible to be distinguished in the fluorescence microscope. Fluorescent polystyrene particles were easily differentiated from algal nuclei according to the following features: NPs had a brighter and lighter shade of blue than the stained nuclei, and they were exceptionally round compared to nuclei in addition to their constant 1 µm size. Physical contact of NPs with protist cells was recorded as adherence. These ten fields of views at 20x magnification of 0.25 mm^2 were chosen randomly, however still systematically covering the entire filter area. Several variables were measured for all present algal cells: number of individual cells and the number of cells per chain for colony-forming algae (Thalassiosira, Chaetoceros, Phaeocystis, other centric and

pennate diatoms). The number of adhered NPs per cell or chain was assessed separately for the abovementioned protist groups by carefully focusing through the entire field of view. Adherence was recorded when the NP was clearly in direct contact with the cell or a component of it, i.e., touching the cell from the sides or being under or on top of the cell, or external structures (Figure 5).

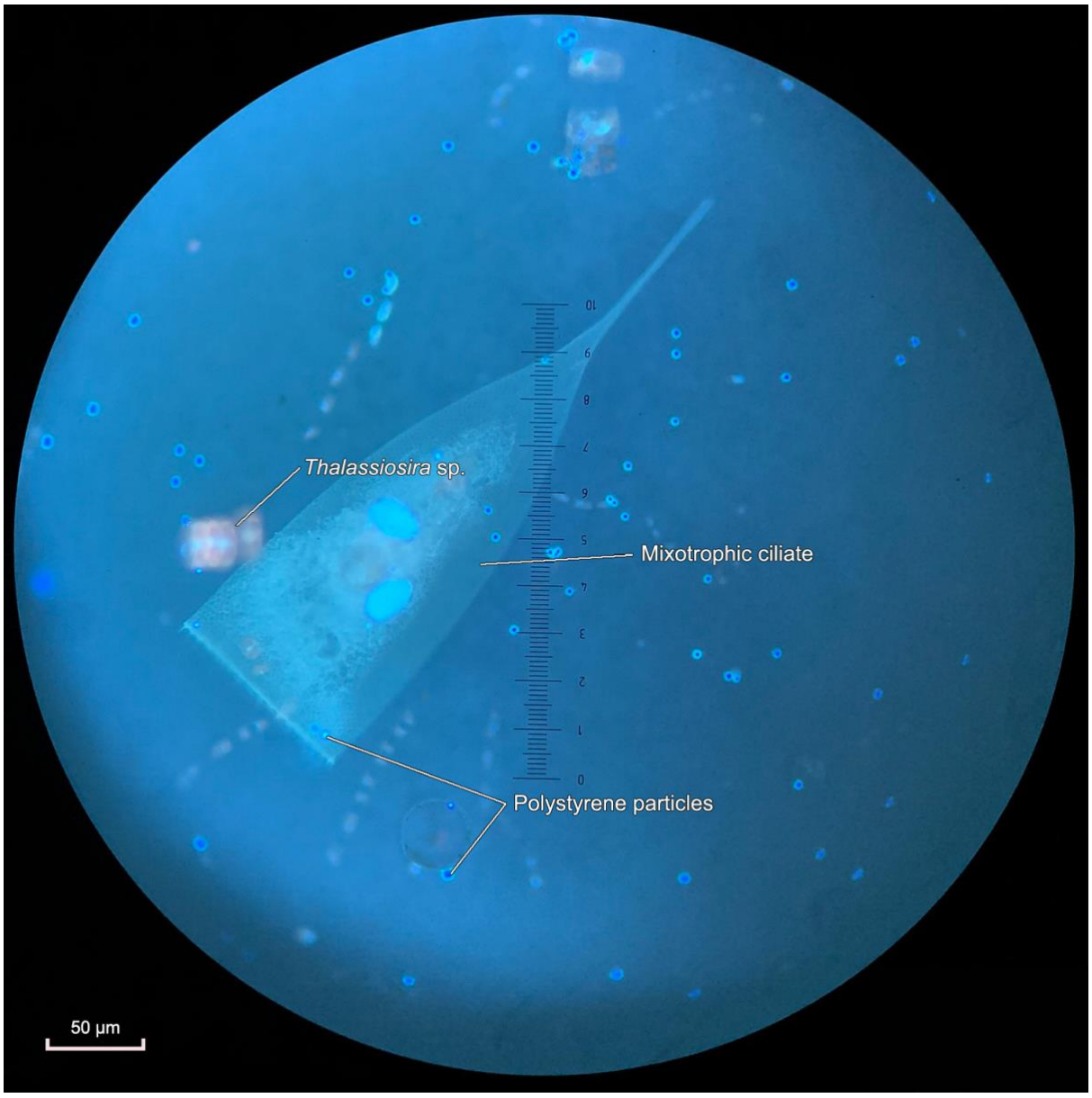

Figure 4a: Example of a sample.

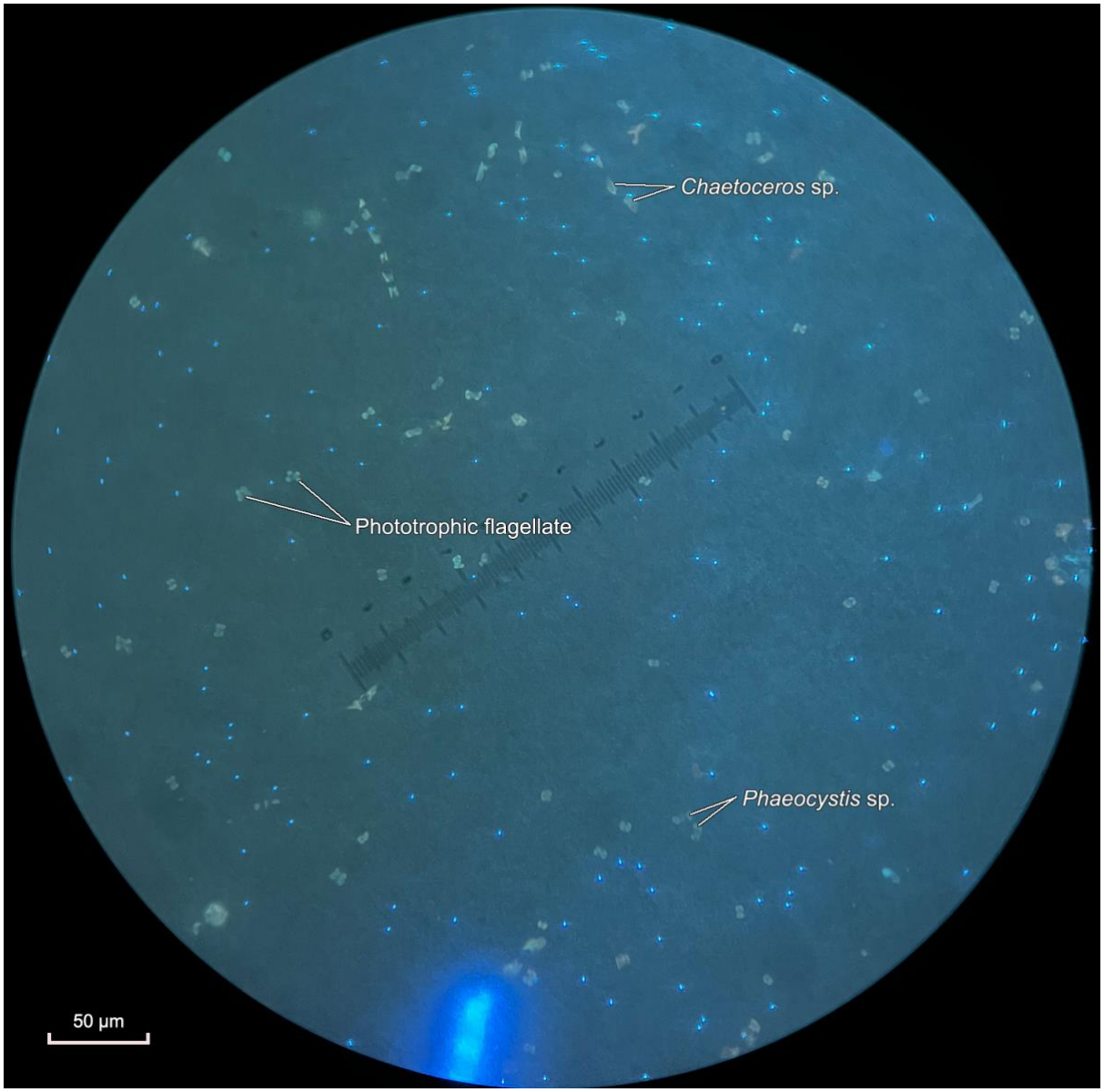

Figure 4b: Example of a sample.

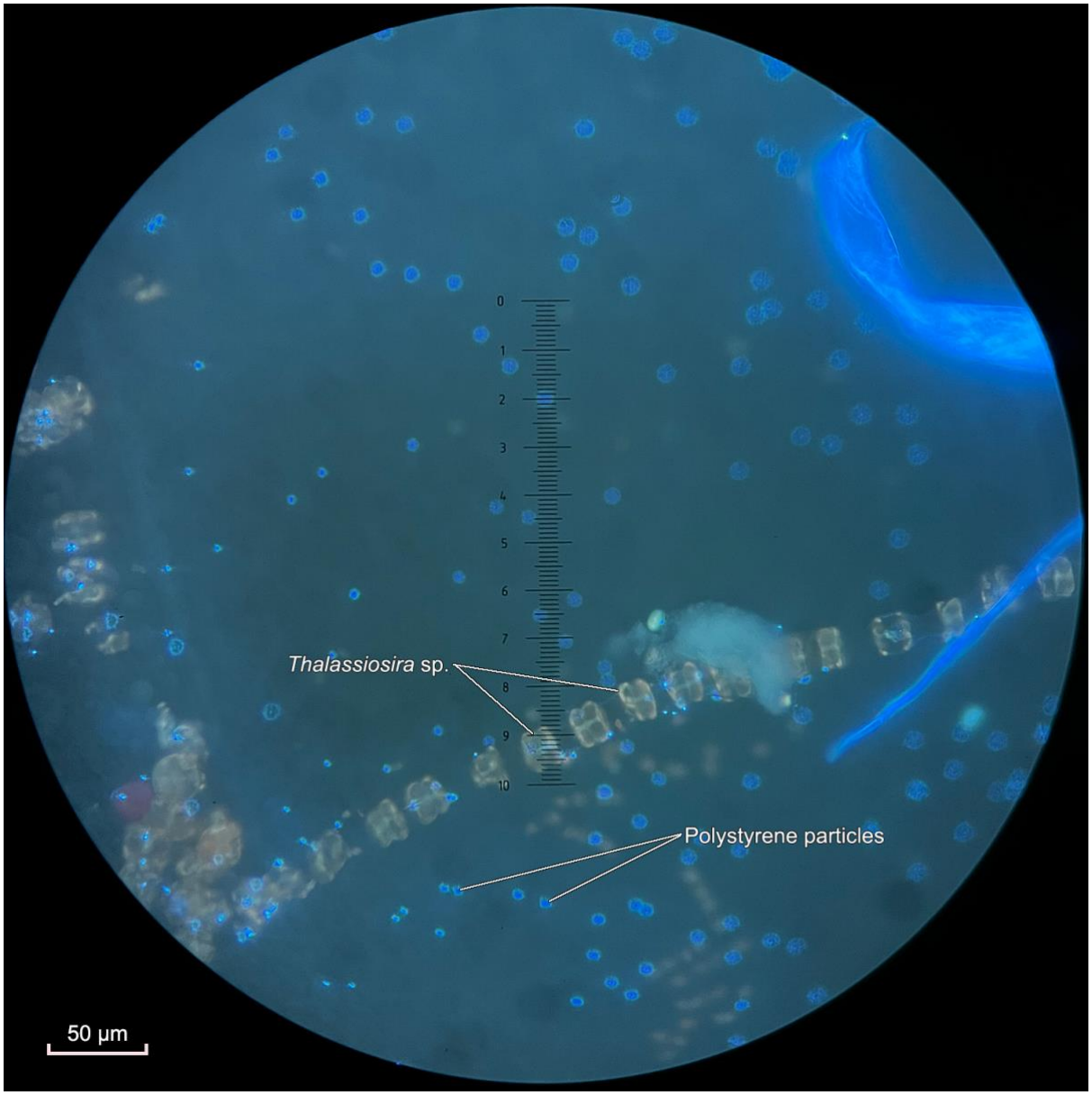

Figure 4c: Example of a sample.

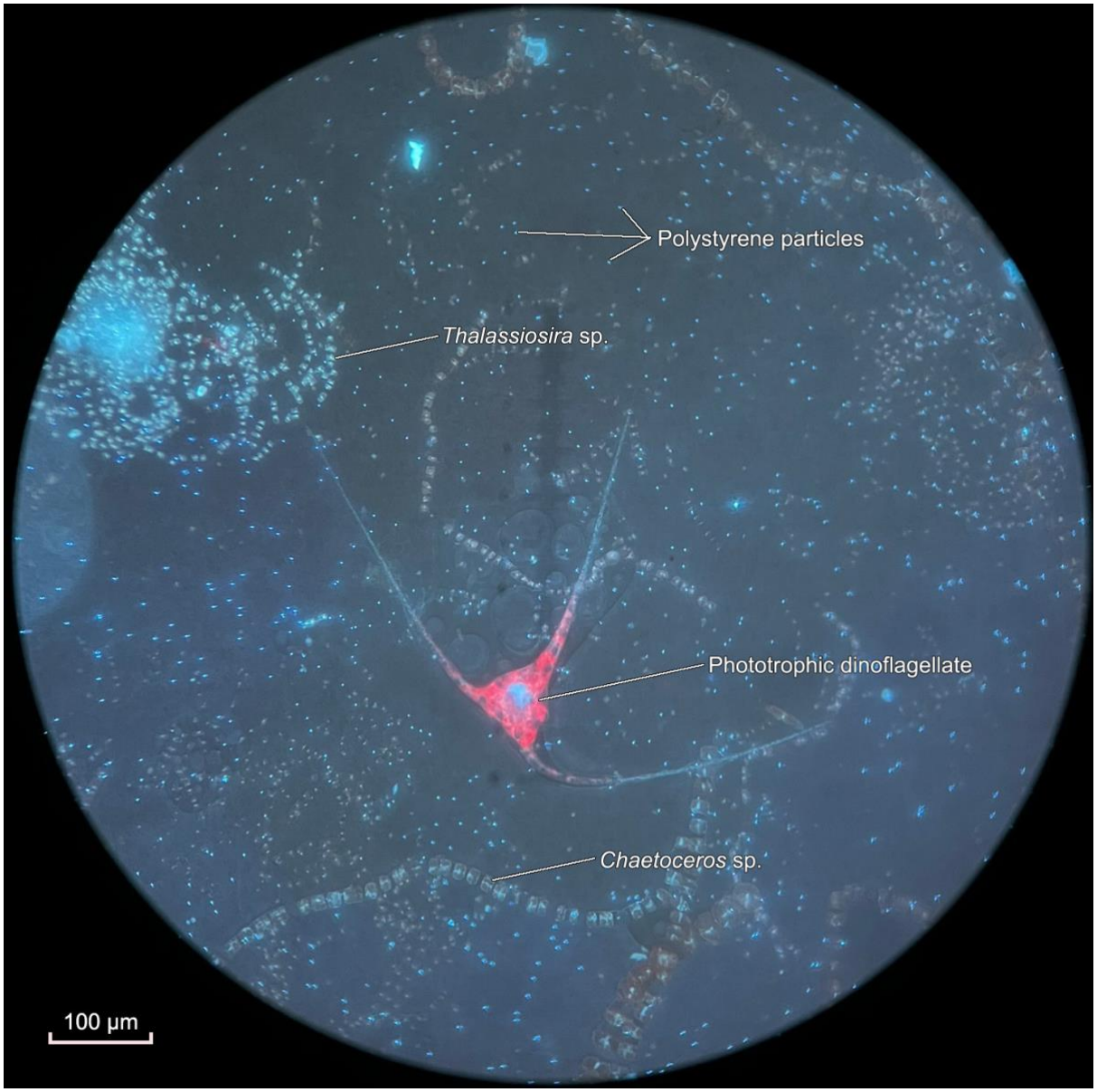

Figure 4d: Example of a sample.

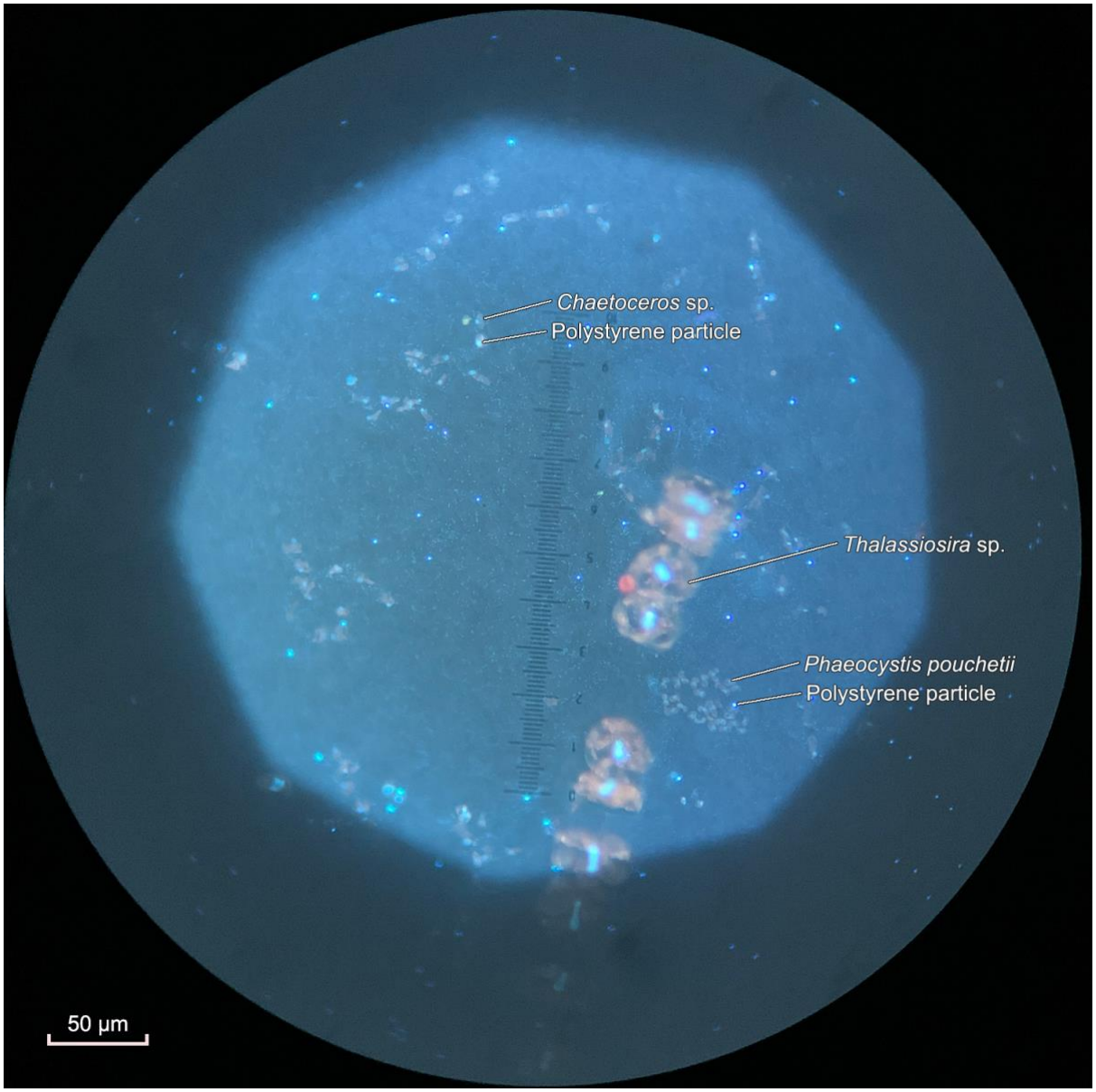

Figure 4e: Example of a sample.

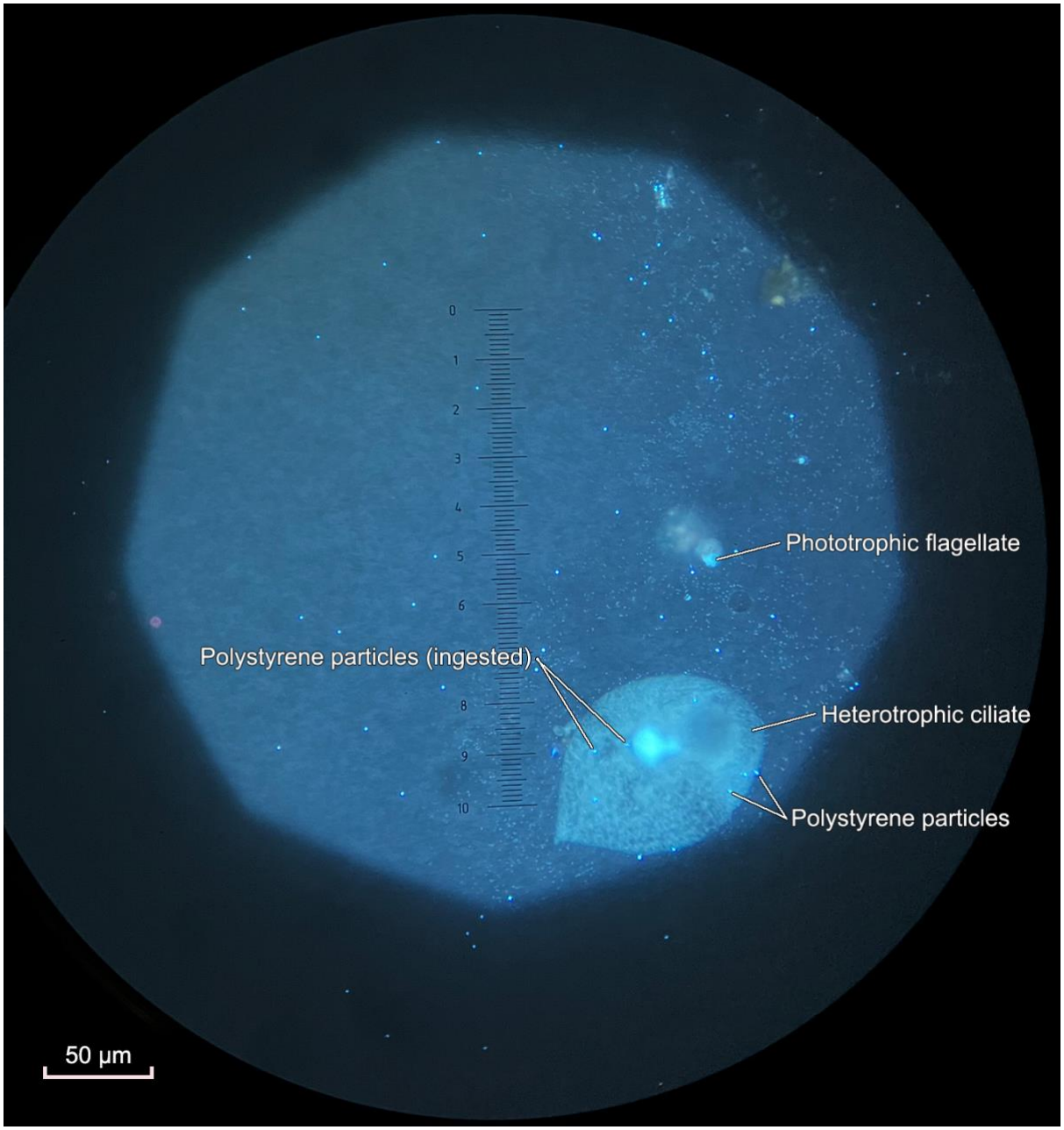

Figure 4f: Example of a sample.

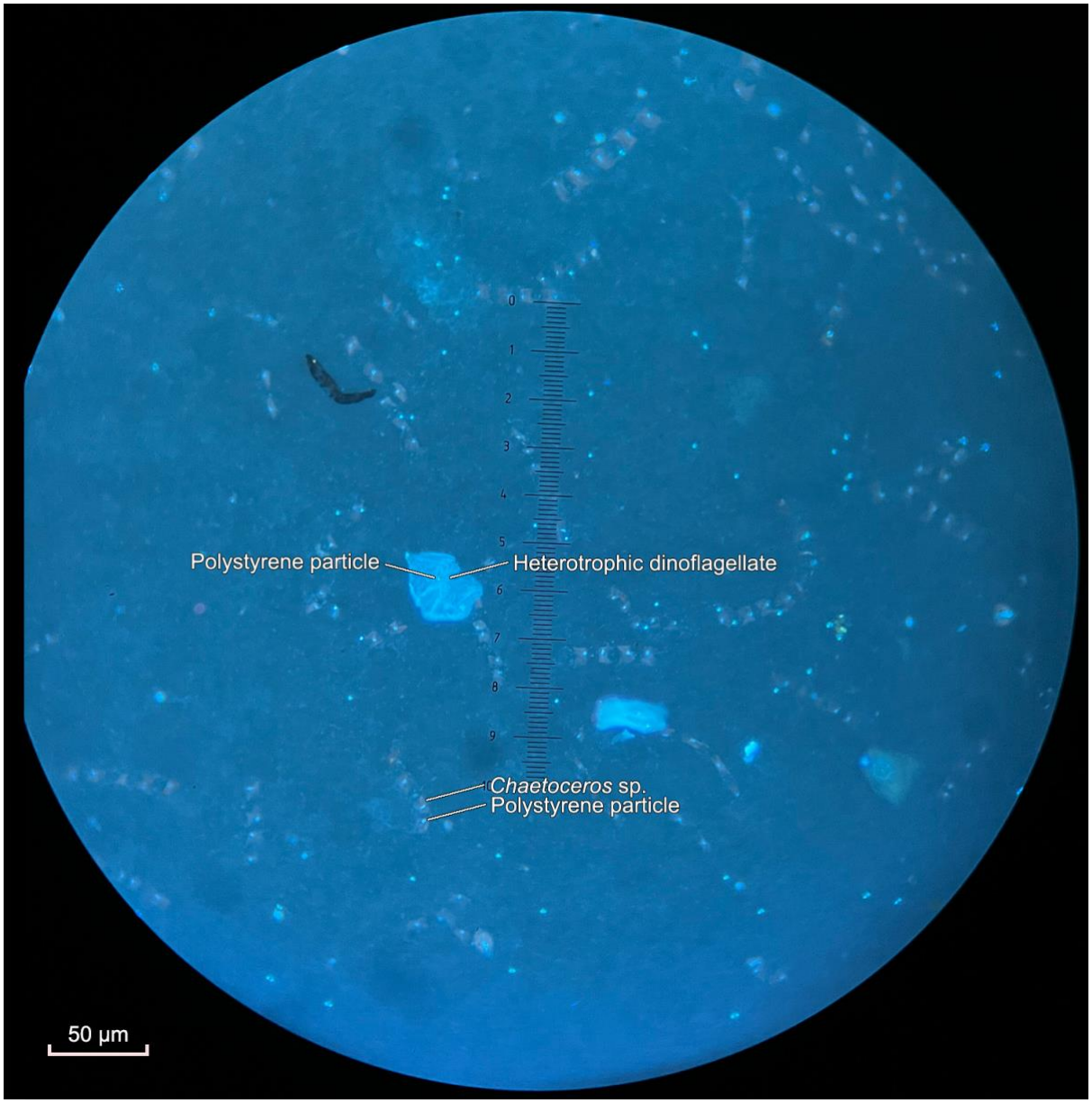

Figure 4g: Example of a sample.

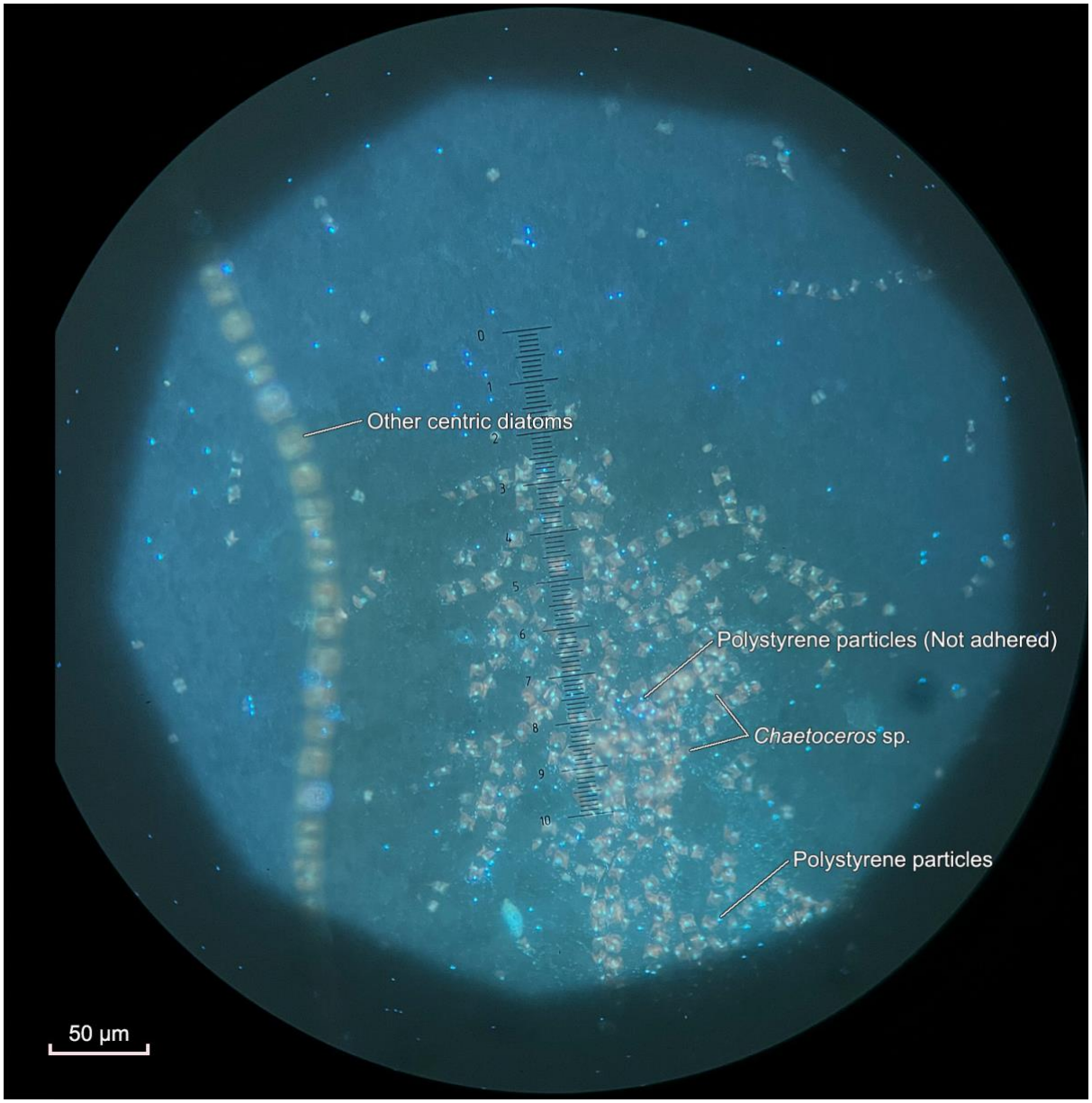

Figure 4h: Example of a sample.

2.2.6. Measurements of TEP in phytoplankton communities

To assess for the potential stickiness of the phytoplankton communities, the concentration of TEP was measured. Immediately after starting the NP exposure experiment (see Section 2.1.4.4.), three additional 200 mL replicate seawater samples from the same Niskin bottles were filtered for this analysis at each sampling station. The samples were filtered through 0.4 µm PC filters at approximately 200 mbar, with a Whatman 0.7µm GF/F filter underneath for

support. After complete filtration, the filter was first rinsed with air, then with 5 mL MilliQ water, followed by a rinse with air to remove all salt crystals. Each PC filter was individually placed in a 1.5 mL Eppendorf tube and stored frozen at -20 °C in darkness until further analysis.

Concentration of TEP was determined with a modified method (Ulrike Dietrich, UiT) from Arruda Fatibello et al. (2004) using Alcian blue stain and calibration relative to Xanthan Gum concentration. Briefly, the 0.4 µm PC filters were transferred to 15 mL Falcon tubes with 5 mL MilliQ water, vortexed and sonicated for 60 minutes (Clifton™ Heated Timed Ultrasonic Bath). After sonication, 4 mL sample was transferred to a new 15 mL Falcon tube with 75 µL acetic acid and pre-centrifuged Alcian blue stain (1 g L^{-1}) (Eppendorf Centrifuge 5702R, 3000 g for 30 min). The mixture was incubated for 10 min at room temperature in the dark and then centrifuged for 30 min. Absorption was measured using a double beam spectrophotometer (UV-6300 PC) at 610 nm wavelength, with Gum Xanthan reference solutions from 0.25 to 10 mg L^{-1} used for calibration.

All environmental variables including ocean temperature, salinity, chlorophyll a and nutrient concentrations were provided by the 2021 Polarfront Cruise science consortium (Gradinger et al. unpubl.)

2.3. Data-analysis

Data-analysis and visualization was mainly conducted using Python (version 3.8.5). Codes were written for all statistical analyses. Station maps and isoline plots were made using Ocean Data View (version 5.6.3). Plots related to algal abundances, NP adherence and TEP made with Python. Nutrient plots made with Excel (version 16.66.1).

To test for species-specific differences in the attachment of the NPs to algal cells a Kruskal-Wallis test by rank was performed, as the assumptions of normal distribution and homogeneity of variances were not met for all variables (Shapiro-Wilk test, Levene's test, p-value < 0.05). A subsequent post-hoc Dunn's test for pairwise comparisons was selected with the most conservative Bonferroni correction of p-values. Spearman's rank correlation test was used to test for monotonic association first between TEP concentration and protist cell abundance, and

later between TEP concentration and number of adhered NPs to algae. Significance was set to a p-value ≤ 0.05.

3. Results

First, the results from monoculture experiments are demonstrated first. Unfortunately, several variables in this study did not provide reasonable results, specifically regarding the particle adherence, and the potential causes are provided in the discussion. Results from field experiment are presented thereafter.

3.1. Estimation of NP adherence in monoculture experiments

Growth curves for Chaetoceros gelidus and Thalassiosira gravida were quite different. Growth curves for both species had no clear deviations between treatments. In C. gelidus, abundances in all treatments increased up to day 3-5, and slowly decreased afterwards (Figure 1a). Therefore, the exponential phase of C. gelidus was short and cells entered stationary phase rapidly (after day 5). Highest algal concentrations were reached on day 5 at $35x10^6$ cells L^{-1} in control and high silica treatments. For T. gravida, growth was slower, and was not clearly separated into exponential and stationary phases (Figure 1b). Here, the highest cell concentration ($1.6x10^6$ cells L^{-1}) was reached on day 10 (after the last full sampling of all variables) in control bottles. Concentrations did not show increases at day 13 which could potentially indicate the beginning of a stationary phase. Unfortunately, neither of the nanoparticles were found in any of the stained samples during microscopic inspection, thus, the data of the experiment were not analyzed further.

3.2. Results from Arctic phytoplankton community exposures

3.2.1. Environmental characteristics in the study area

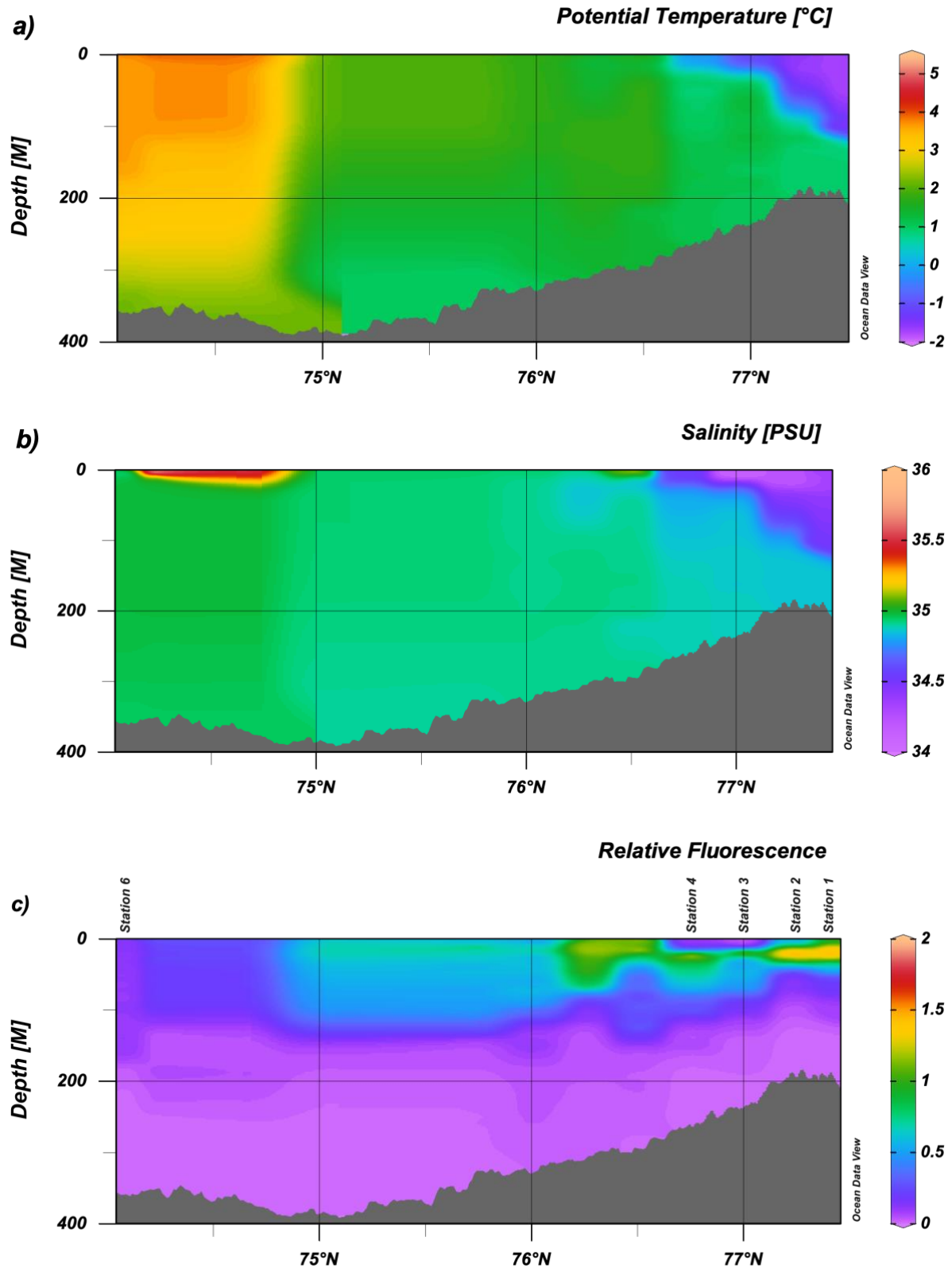

Figure 5: Physical properties across the study sites, showing a) potential temperature (°C), b) salinity (psu), and c) relative algal chlorophyll fluorescence. Data from the CTD Rosette casts. Sampling stations of this study are marked in a). To account for pressure differences in the ocean between varying depths, potential temperature was used.

The hydrographical data show a clear separation between AW in the south and ArW in the north at the surface. In the north (Stations 1-3), where marginal ice zone (MIZ) conditions were present, surface water temperature was approximately between -1.7 and -0.4 °C, and salinity between 34.3 and 34.6 psu. This cold and relatively fresh, stratified water at the surface was ArW with meltwater from sea ice, while AW was located underneath. At Station 4 the surface temperature increased to around 0.6 °C with a salinity of 34.7 psu. Between Stations 4 and 6 both surface salinity and temperature remained stable, approximately 1.5 °C and 34.8 psu, respectively. At the southernmost station, surface temperature was 3.7 °C and salinity 35.0 psu, which indicated typical values of AW with higher salinity and temperatures. The Polar Front was approximately located at Station 3.

Higher algal chorophyll fluorescence was found in the relatively cold and fresh and stratified Arctic waters. A clear maximum was very distinct and strongest for the whole transect at Stations 1 and 2 with a the peak was between 15 and 25 m. Stations 3 and 4 had very low surface fluorescence by maxima in 20 (Station 3) and 25m (Station 4). In the AW Station 6, fluorescence was very low throughout the whole water column, including at the surface.

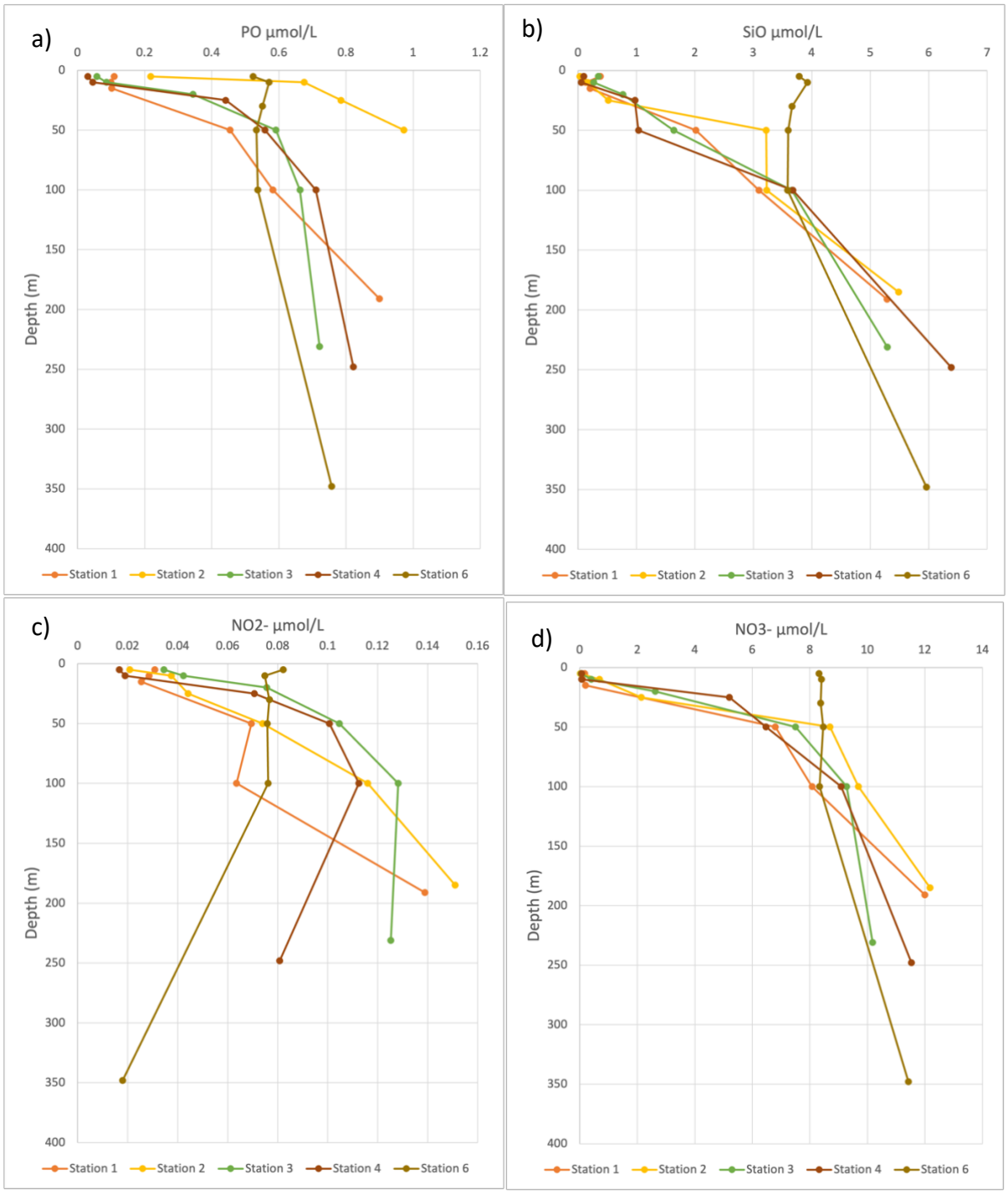

Figure 6: Nutrient concentrations of a) phosphate (PO_4^{3-}), b) silicate ($Si(OH)_4$), c) nitrite (NO_2-) and d) nitrate (NO_3-) (µmol L^{-1}) at each station.

Nutrient concentrations at the four northernmost stations were low in the surface waters (>50 m) in the regions of high chl fluorescence and increased along the depth. However, in the low chlorophhyll fluorescence Station 6, all nutrients were abundant throughout the whole water column. This created a gradient with lowest values at Station 1, similar patterns at Stations 2-4 and highest concentrations in Station 6 in the sampling depths (Chl a max).

3.2.2. Protist abundance and species composition

Total algal abundances (Figure 7a) ranged from 6.17 ± 2.19x10^6 cells L^{-1} to 9.24 ± 0.54x10^5 cells L^{-1} and differed significantly between stations (Kruskal-Wallis test, p-value < 0.05) with the lowest abundance occurring at Station 6 and the highest at station 4. While not all taxa could be identified to species level, this was possible for Chaetoceros gelidus and Phaeocystis pouchetii, which both dominated in their genera. Overall, the most abundant taxa were Thalassiosira spp., Chaetoceros spp. and Phaeocystis pouchetii (Table 4, Fig. 7b). Thalassiosira spp., heterotrophic dinoflagellates and all ciliates had their highest relative abundances in Station 1 while it was lowest for Phaeocystis pouchetii (Table 4). Other protist groups were moderately abundant in that station. Stations 2 and 3 were quite similar, except other centric diatoms had their highest abundance in Station 2, while pennate diatoms and phototrophic dinoflagellates were highest in Station 3. Additionally, in the latter station, there were no recordings on other centric diatoms, heterotrophic ciliates and flagellates. Highest total abundance of phytoplankton was recorded in Station 4, where Chaetoceros spp., Phaeocystis spp. and phototrophic flagellates had their highest abundances. Algal abundances at Station 6 were an order of magnitude lower than at Station 4. While the groups Thalassiosira spp., Chaetoceros spp. and phototrophic dinoflagellates had their lowest abundances here, it was highest for heterotrophic flagellates.

For colony-forming taxa, observed colony sizes ranged from single cells to 9.5 ± 3.7 cells/colony (Table 4). Thalassiosira spp. had the longest chains while they were shortest for other centric diatoms. Highest Phaeocystis spp. colony size was seen at Station 2, with 4.9 ± 4.7 cells/colony.

Table 4: Hydrographic conditions and protist abundances (10^3 cells L^{-1}; mean and standard deviation) in the experimental treatments.

	Station 1	Station 2	Station 3	Station 4	Station 6
Water mass	ArW	ArW	ArW	AW	AW
Sampling depth (m)	15.0	25.1	20.0	25.3	30.5
Temperature (°C)	- 1.75	- 1.53	- 0.37	0.59	3.69
Salinity (PSU)	34.35	34.28	34.57	34.75	34.98
Thalassiosira spp. abundance	698 ± 2	195 ± 27	251 ± 97	262 ± 89	29 ± 20
Thalassiosira spp. average colony size (cells/colony)	8.34 ± 3.38	4.29 ± 2.45	9.50 ± 3.71	7.44 ± 5.53	1.67 ± 0.59
Chaetoceros spp. abundance	2559 ± 426	3624 ± 1790	2946 ± 576	4348 ± 1862	156 ± 40
Chaetoceros spp. average colony size (cells/colony)	5.23 ± 0.18	3.81 ± 0.99	4.57 ± 1.20	4.99 ± 1.52	3.11 ± 3.95
Phaeocystis spp. abundance	59 ± 15	694 ± 536	688 ± 80	1178 ± 386	425 ± 82
Phaeocystis spp. average colony size (cells/colony)	1.59 ± 1.01	4.90 ± 4.71	1.18 ± 0.15	1.19 ± 0.08	1 ± 0
Other centric diatoms abundance	6 ± 6	88 ± 56	0	0	3 ± 4
Other centric diatoms average colony size (cells/colony)	1.50 ± 1.06	6.67 ± 4.71	0	0	2 ± 1.15
Pennate diatoms abundance	18 ± 18	35 ± 18	78 ± 69	20 ± 14	16 ± 4
Pennate diatoms average colony size (cells/colony)					
Phototrophic dinoflagellates	66 ± 26	23 ± 4	90 ± 0	15 ± 3	13 ± 7
Heterotrophic dinoflagellates	9 ± 4	1 ± 2	1 ± 2	0	1 ± 2
Mixotrophic ciliates	37 ± 33	16 ± 4	9 ± 6	4 ± 3	18 ± 4
Heterotrophic ciliates	20 ± 2	6 ± 5	0	0	1 ± 2
Phototrophic flagellates	N/A	119 ± 66	54 ± 26	312 ± 99	213 ± 84
Heterotrophic flagellates	N/A	23 ± 33	0	33 ± 14	48 ± 10
Total abundance of centric diatoms	1088 ± 1106	1032 ± 1941	1066 ± 1376	1537 ± 2264	63 ± 72
Total abundance of algae	3472 ± 385	4826 ± 1367	4036 ± 640	6174 ± 2189	924 ± 54

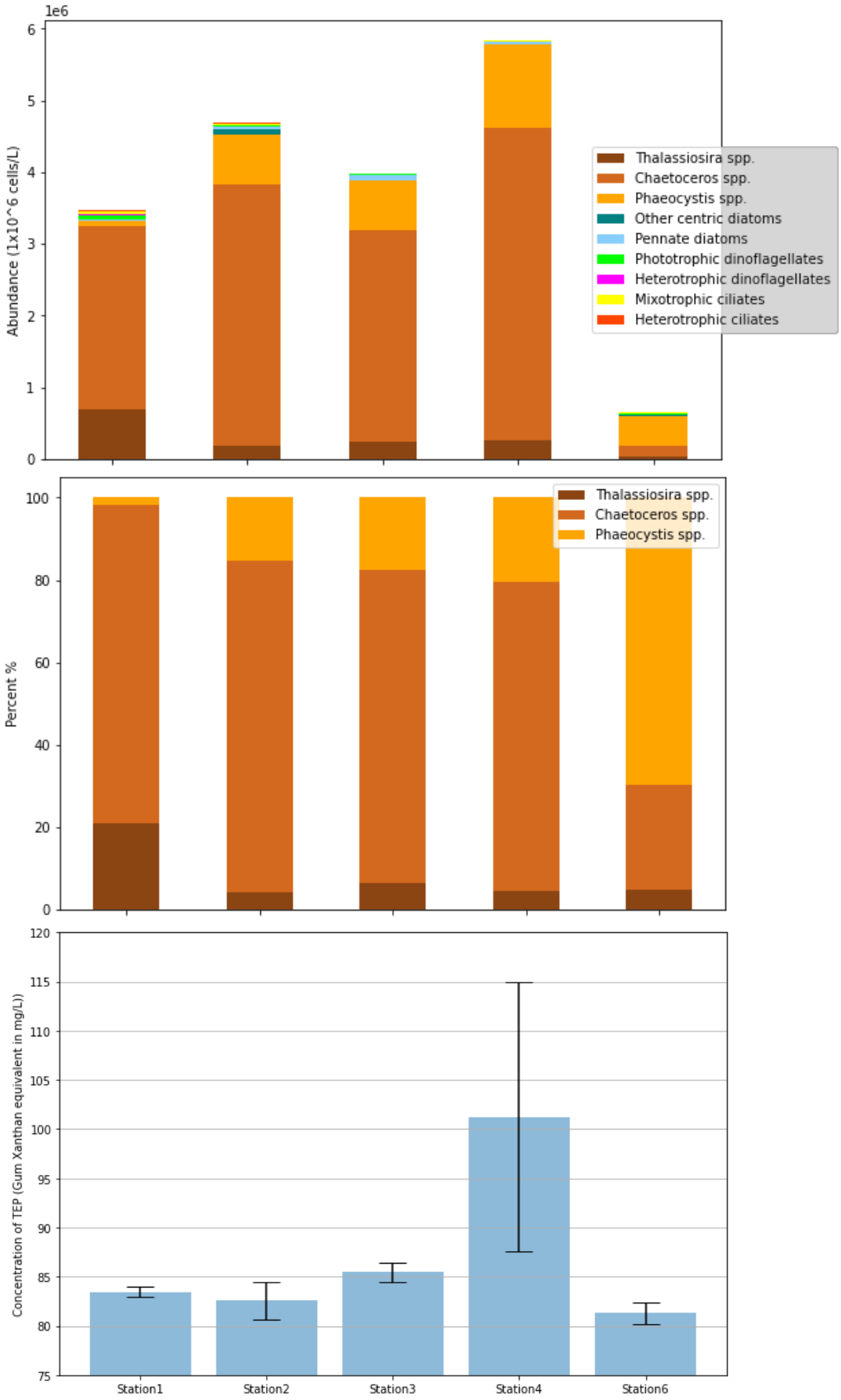

Figure 7: a) Total protist abundance in cells L^{-1}, b) relative abundance of the three most abundant groups, and c) concentration of TEP expressed as Gum Xanthan equivalent (mg L^{-1}).

Station 4 had the highest abundance of the three major taxonomic groups (Thalassiosira spp., Chaetoceros spp. and Phaeocystis spp.; Table 4), and the drop in relative abundance of diatoms was clear in Station 6 (Figure 7b). In the four northern stations Chaetoceros spp. was clearly dominating the community, contributing almost 80 % of relative abundance between the three groups. Thalassiosira spp. relative abundance was highest at Station 1 was over 20 %, and approximately 5 % at the other stations. Relative abundance of Phaeocystis spp. increased southwards with a high proportion at Station 6 (approximately 70 %). There was no statistically significant difference between abundances of protist groups between Arctic and Atlantic stations except for phototrophic and heterotrophic flagellates (Kruskal-Wallis test, p-value < 0.05), however no significant results were shown in the Dunn's post-hoc test.

TEP concentrations were similar between stations except for Station 4 (Figure 7c). At all stations, the average concentration was over 80 GX eqv. mg L^{-1} and highest at Station 4 the concentration exceeding 100 GX eqv. mg L^{-1}.

3.3.3. Adherence of NP particles to phytoplankton and concentration of TEP

Only a fraction of the nominal NP concentration placed in the treatment bottles was found after the 3 h incubation. While the targeted concentration of polystyrene NPs was 10 000 particles mL^{-1}, the recovery concentration obtained after incubation was $4.8 \pm 1.4x10^6$ beads L^{-1}. Of this number, $3.3 \pm 7.1x10^4$ beads L^{-1} were adhered to protists, which means that 0.7 % of all beads detectable after 3hours were adhered to protists.

Almost all protist groups (excluding heterotrophic dinoflagellates) showed some adherence of NPs after the 3h exposure however in significantly different amounts (test of total abundances between protist groups, Kruskal-Wallis test, p-value < 0.05). On average 9.1% of all protist cells abundance had adhered NPs, and the average NPs per cell was 0.09. The level of adherence across all protists ranged from 1.4 to 83.7 %. The highest adherence in diatoms occurred in Thalassiosira spp. (37.4 %) and lowest in Chaetoceros spp. (5.8 %; see also Table 5, Figure 8). Pennate and other centric diatoms showed similar intermediate adherence levels of 15.5 and 15.4 %, respectively. The highest fractions of cells with NPs adhered occurred for mixotrophic (83.7 %) and heterotrophic ciliates (64.3 %), and the lowest for phototrophic (2.6

%) and heterotrophic flagellates (1.4 %). About 6.5% of the Phaeocystis spp. cells had adhered NPs. However, no statistically no statistically significant differences were detected.

A comparison between adherence to single cells versus colonies showed species specific differences. Of all adhered NPs in colony-forming protists, the majority of adherence was with cell colonies in diatoms, while the opposite was true in Phaeocystis spp. For other centric diatoms, only colonies adhered NPs. For Thalassiosira spp., Chaetoceros spp. and pennate diatoms the colony adherence was 94.1, 91.8 and 58.8%, respectively.

Frequently, NPs adhered to centric diatoms, especially Thalassiosira spp. were attached to the corner of the cell or between two cells.

Table 5: Adherence of NPs based on cell abundance (10^3 cells L^{-1}; mean and standard deviation)

	Station 1	Station 2	Station 3	Station 4	Station 6	Mean
Thalassiosira	167 ± 35	90 ± 26	107 ± 33	117 ± 49	23 ± 17	96 ± 56
Chaetoceros	212 ± 66	233 ± 110	204 ± 10	229 ± 171	14 ± 17	176 ± 130
Phaeocystis	2 ± 2	22 ± 24	49 ± 9	145 ± 18	26 ± 8	52 ± 53
Other centric diatoms	2 ± 2	13 ± 10	0	0	0	3 ± 7
Pennate diatoms	4 ± 4	16 ± 14	1 ± 2	4 ± 3	0	5 ± 9
Phototrophic dinoflagellates	7 ± 7	6 ± 8	1 ± 2	0	1 ± 2	3 ± 5
Heterotrophic dinoflagellates	0	0	0	0	0	0
Mixotrophic ciliates	22 ± 9	12 ± 9	7 ± 10	0	26 ± 16	13 ± 14
Heterotrophic ciliates	20 ± 20	0	0	0	0	3 ± 10
Phototrophic flagellates	NaN	3 ± 4	7 ± 5	2 ± 3	6 ± 8	5 ± 6
Heterotrophic flagellates	NaN	0	0	0	1 ± 2	0.3 ± 1

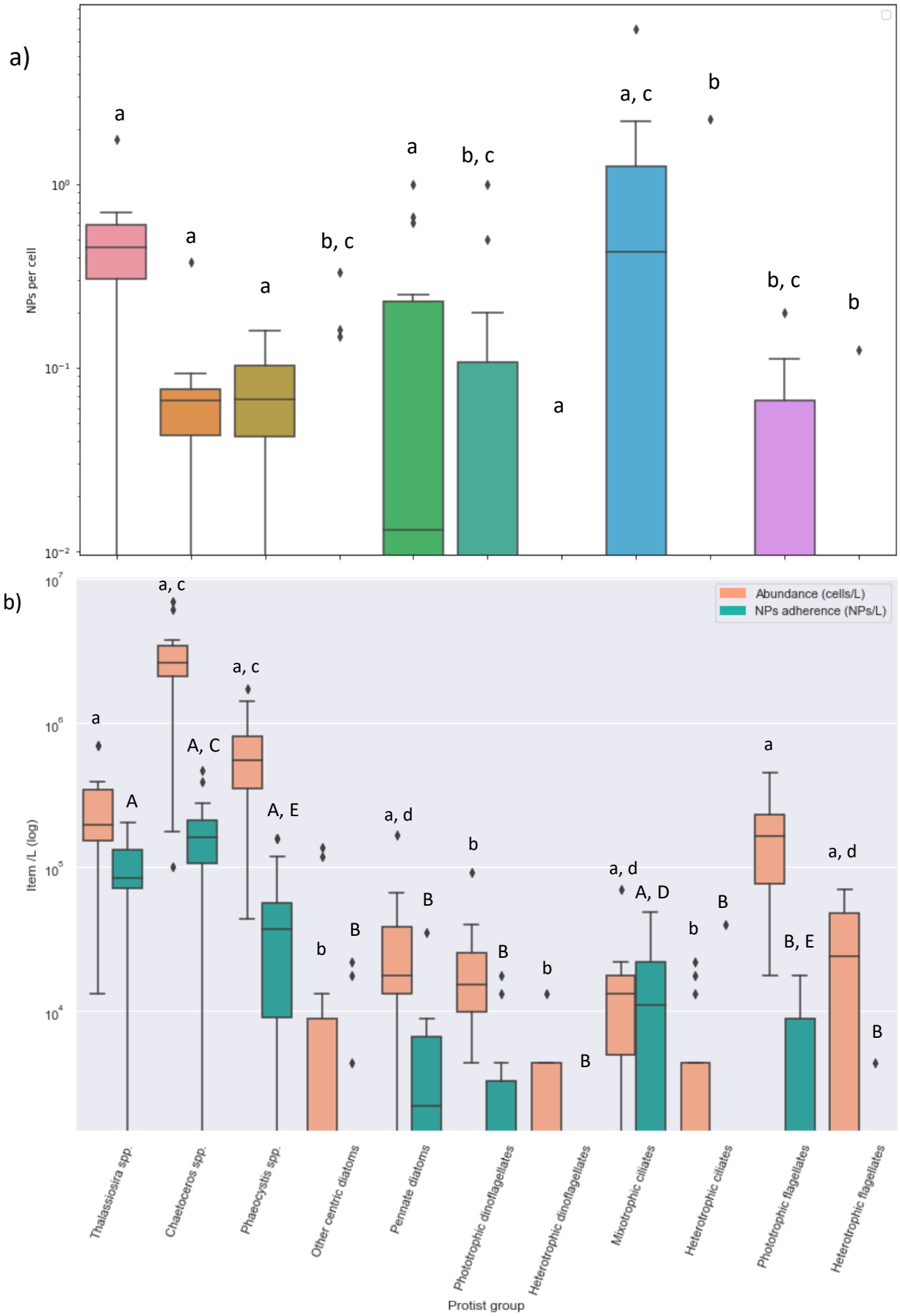
a)
NPs per cell
10^{0}
10^{-1}
10^{-2}
a
a
a
b, c
a
b, c
a
a, c
b
b, c
b
b)
Item /L (log)
10^{7}
10^{6}
10^{5}
10^{4}
Abundance (cells/L)
NPs adherence (NPs/L)
a
A
a, c
A, C
a, c
A, E
b
B
a, d
B
b
B
b
B
a, d
A, D
b
B
a
B, E
a, d
B
Thalassiosira spp.
Chaetoceros spp.
Phaeocystis spp.
Other centric diatoms
Pennate diatoms
Phototrophic dinoflagellates
Heterotrophic dinoflagellates
Mixotrophic ciliates
Heterotrophic ciliates
Phototrophic flagellates
Heterotrophic flagellates
Protist group

Figure 8: a) Number of adhered particles per cell per group. Notice the log scale. Outliers shown in each figure. b) Total abundance of protist groups (cells L^{-1}) with the respective total number of adhered NPs in each group (particles L^{-1}). Logarithmic scale. Statistically significant (Kruskal-Wallis test, p-value < 0.05) differences shown with different letters, i.e. groups with same letter are not different from each other, while e.g. group a was significantly different from b etc.

Adherence between protist groups was statistically significantly different (Kruskal-Wallis test, $p < 0.05$), and several paired groups had significant differences in their NP adherence levels (Dunn's test p-value < 0.05; marked with letters in Figure 8). Moreover, total adherence of NPs between stations was statistically significant based on Kruskal-Wallis test, however no significance was detected in Dunn's post-hoc test.

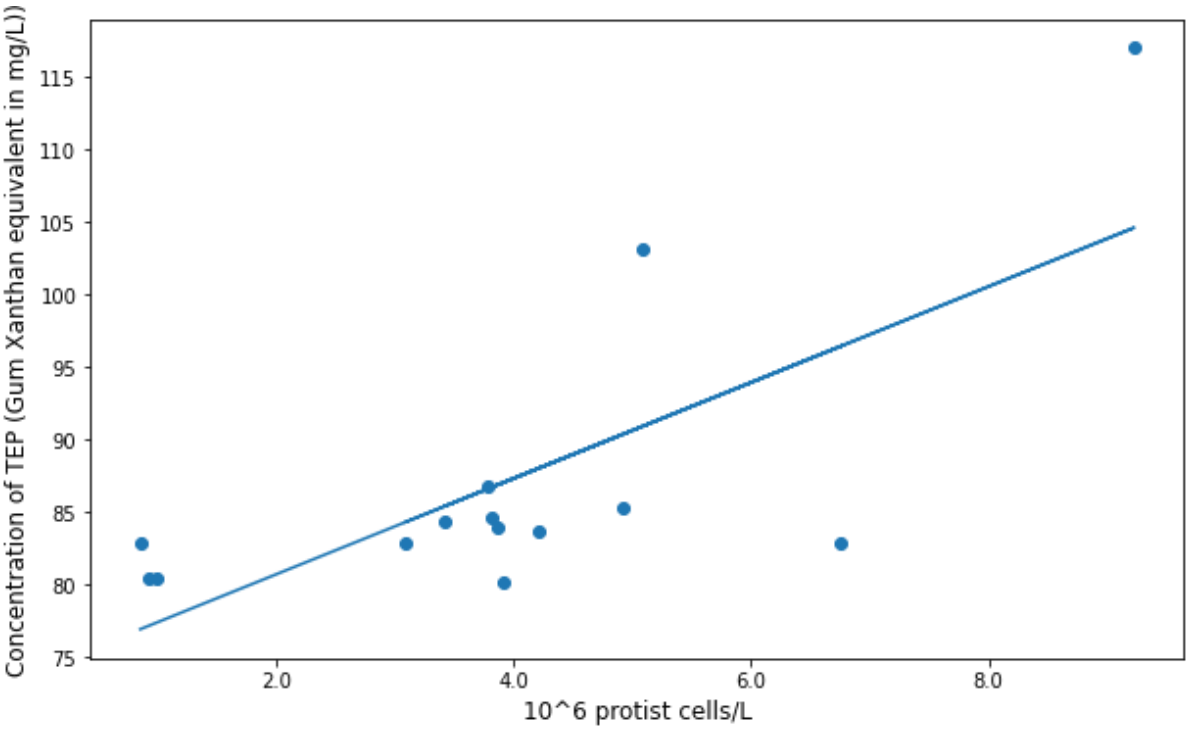

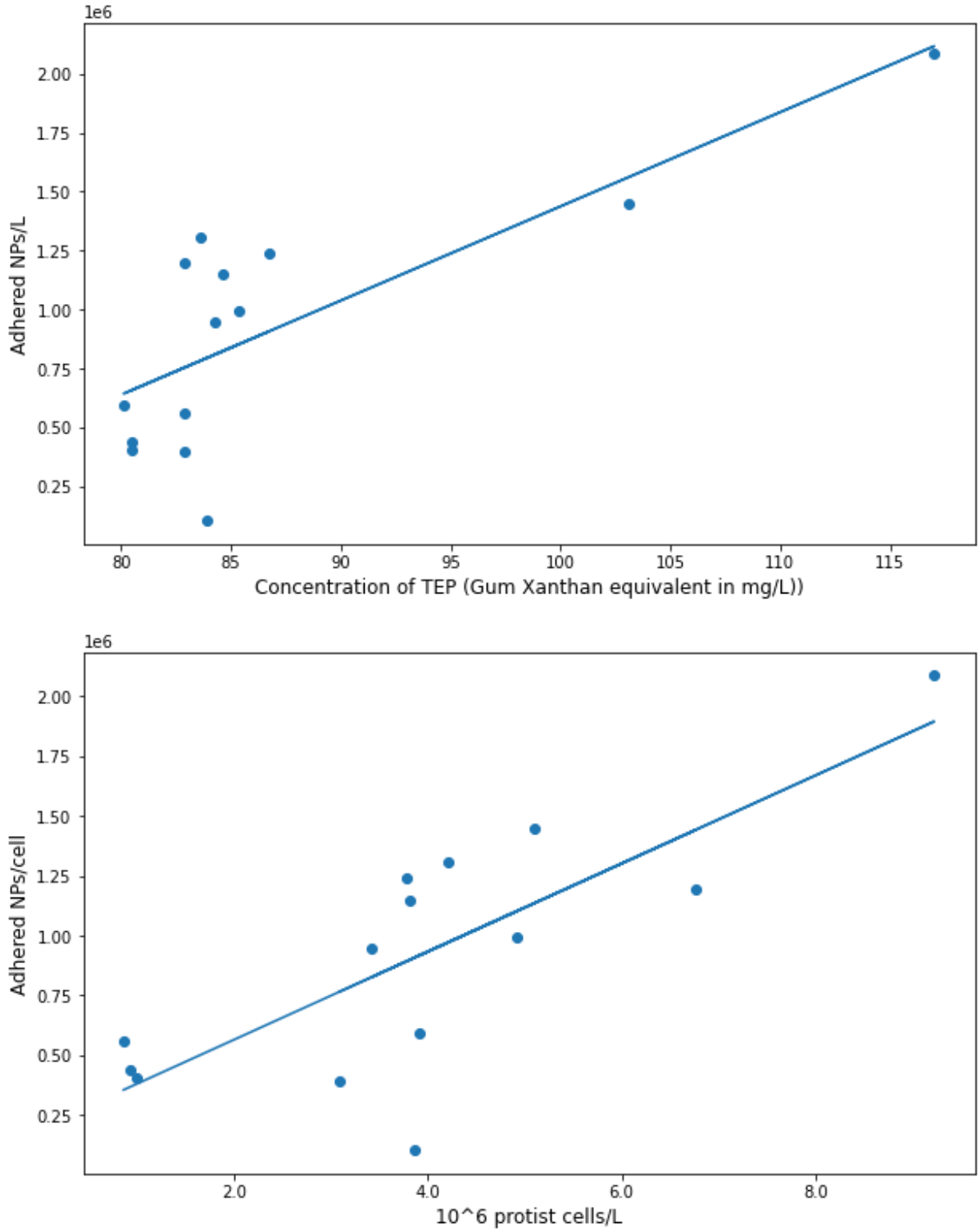

Figure 9: Linear regression between a) TEP and protist cell abundance (R^2 = 0.53, y = 74 + x0.000003, b) TEP and adhered NPs (R^2 = 0.59, y = -2560000 + x40000), and c) protist cell abundance and adhered NPs (R^2 = 0.61, y = 198877 + x0.18).

The concentration of TEP were not clearly correlated to protist cell abundances, as well as the total number of adhered NPs with TEP concentration. Highest adherence occurred combined with high TEP concentration and protist abundance. Spearman's rank correlation test showed no significant monotonic correlation between TEP and protist abundance, nor TEP and adherence of NPs. Finally, the number of adhered NPs was positively related to the abundance of protists and adhered particles indicating the importance of particle encounter rates (Figure 9c).

4. Discussion

This is the first study exposing sub-Arctic algal communities and species to NPs. Unfortunately, unexpected problems with the single species experiments like disappearance of the particles limits the scientific outcome of the study and only possible explanations for the shortcomings and suggestions for experimental improvements can be discussed and provided.

The mixed Arctic phytoplankton community experiments from the Barents Sea Polar Front successfully tested adherence to polystyrene NPs at a taxon specific level. Species-specific adhesion was confirmed but the results contrasted the initial hypothesis that TEP production would be a major factor. Here the discussion will provide further explanations of the results, and their relevance in the ecology of the Polar Front region.

4.1. Shortcomings of the monoculture exposures to NPs

In the laboratory study of adherence in single-species diatom cultures, the polystyrene NPs added to the exposure bottles could not be located at the end of the incubation. Adherence rates could therefore not be determined in conjunction with growth rates. This error may be due to the following factors. First, while the description of the fluorescent polystyrene particles state that there is little to no photobleaching even under intense UV-light, this was the most obvious concern in our work. The packaging indicated that the contents should still be protected from light, but between these two pieces of information there is not a timeline for when decaying of the dye would start approximately. The exposure length was up to 13 days long, where the first sampling done on day 4. No particles were found in any treatment, sampling day nor species, which was true for both PS and Si particles. Cellular internalization, like observed in (Y. Chen et al., 2020), could not occur to a level of nearly 100 % of the particles in the whole population, and on top of this, fluorescent particles could still be observed from within the cells, just like the nucleus and chloroplasts. Plastic degradation by phytoplankton has not been observed to any extent yet, which makes it also an unlikely option for the disappearance of the nanoparticles.

Another experiment was set up to try to assess the possible errors. The following trouble shooting steps were attempted with ASW using the same particle concentration, experiment setup, treatment bottles and filtration step according to the experiment (see Section 2.1.4.4.) and inspection of the filtrations were done with the same fluorescent microscope.

1. Fluorescent dye decays under exposure to constant light. Over the course of 5 days, NPs in ASW were exposed to the exact light conditions of the experiment, and a subsample was filtered daily to see the possible steps of decay.
2. Beads aggregate strongly in seawater. The same procedure was followed as step 1, but with MilliQ.
3. Beads adhere strongly to the bottle walls. The same procedure was followed as step 1, but it was done under dark conditions.
4. Errors in dilution steps. First, stock solution fluorescence was assessed by pipetting 5 µL directly from the stock solution onto a clean microscope slide with a cover glass on top. Second, working solution was made according to the single species experiment. A subsample of this working solution was filtered. Third, working solution was diluted into the final experiment concentration, and a subsample was filtered of this.

Steps 1-3 did not yield any results. No particles were detected in any of these subsamples, anywhere from day 0 until day 5. For step 4, particles were found in the stock solution for both materials, however, only the PS working solution had detectable particles, but in final experimental solution particles were not present for either polymer type. It is noteworthy that even though Si beads were visually observed from the stock solution sample, the fluorescent dye decayed in a matter of seconds from exposing them to UV-light. This indicates that the dye in these particles was clearly more unstable than that of polystyrene, which remained visible after one minute. Because of these results, the most likely option was particles were not transferred from working to final solutions, or that adherence to treatment bottle walls was instantaneous, which seems unlikely. Additionally, after this single species experiment, another one was done with natural Arctic phytoplankton communities, in which the same setup and equipment were used, except that exposure time was only 24 h and incubation took place in the dark. There, particles were clearly fluorescent and within expected concentrations. This leads to the question of whether using ASW instead of (filtered) seawater influences particle behaviour. FSW was not tested due to lack or time, thus, no further trouble shooting steps were implemented.

For future studies, it is suggested that a) particle fluorescence is tested prior to main exposure to confirm or reject the stability of the fluorescent dye, b) different treatment containers are tested for exclude the possibility of intense adherence to the walls, c) different treatment mediums are tested along with the particle fluorescence for influences on particle behaviors.

4.2. Species-specific adherence of NPs in the Arctic phytoplankton communities

4.2.1. Environmental conditions in the study area

The study area had been clearly divided by dominance of AW in the south and ArW in the north, which typically is ice covered as in our study (Slagstad & Støle-Hansen, 1991). Sea ice melt created a pycnocline around 10-15 m leading to a Chl max depth due to stronger stratification and shallower mixing of the water column (Slagstad & Støle-Hansen, 1991). Nutrient depletion as observed at stations 3 and 4 were leading to deep Chl max. Generally, the variability in phytoplankton abundances follows and influences the patterns of nutrient availability at the sea surface (Reid Jr., 1962), with silicate and nitrate as main limiting factors in the Barents Sea (Harrison & Cota, 1991). While nitrate is required by all algae, primary production in diatoms is in addition dependent on silicate, because they require this nutrient to build their frustules made of biogenic silica (bSiO2) (Krause et al., 2018). Therefore, silicate can be a strong limiting factor during diatom blooms in the Barents Sea (Krause et al., 2018; Rey & Skjodal, 1987). Such conditions were encountered in the northern part of the transect, which were dominated by high abundances of diatoms combined with low silicate concentrations indicating a late spring bloom stage in the algal phenology. Additionally, nitrate concentrations were low at Station 1 making it the most nutrient-limited station. No algal growth limitation did occur at station 6 which had highest concentrations of nutrients and the lowest algal abundances.

4.2.2. Spring bloom phytoplankton community composition at the Polar Front

Phytoplankton composition can vary with season. Typical Barents Sea spring phytoplankton blooms for both species and their abundances were observed in the Polar Front area dominated by diatoms, namely Chaetoceros spp. and Thalassiosira spp. Thalassiosira species usually initiate the bloom followed by certain Chaetoceros species (C. von Quillfeldt, 1996). The dominance of Chaetoceros spp. over Thalassiosira spp. in the northernmost stations support the conclusion of a late bloom stage in the spring cycle, in agreement with also the nutrient distributions (C. von Quillfeldt, 1996; C. H. von von Quillfeldt, 2000). Chaetoceros gelidus often dominates the Chaetoceros species in the Arctic, specifically in areas with partial sea ice melt as observed in our study area as far south as Station 3 and excluding the open water Station 6. Phaeocystis pouchetii can be highly abundant in both high and low abundances of diatoms (E. Hansen & Eilertsen, 2007), as was observed throughout the whole study transect. Pennate diatoms were not present in high abundances ($< 1x10^5$ cells L^{-1}) at any station as they can be abundant in early Arctic spring bloom stages in ice covered areas but are then gradually gets replaced by centric diatoms (Grønted & Seidenfaden, 1938; C. von Quillfeldt, 1996) as in our study. Interestingly, the highest total abundance of phytoplankton was observed in Station 4, while relative fluorescence was highest at the two northernmost stations, demonstrating clear separation between fluorescence and abundance. Interestingly P. pouchetii mainly occurred as single cells rather than colonies using the epifluorescence microscopy data, while other studies observed higher fractions of colonies (Rat'kova & Wassmann, 2002). Ciliates were observed mostly in the sea ice melting areas and the southernmost open water station, accordingly with Rat'kova & Wassmann (2002).

This data shows that the Polar Front was not a boundary between Arctic and Atlantic phytoplankton communities but is rather an area for accumulation (Makarevich et al., 2021). A continuum of different stages of the phytoplankton bloom was observed, with late bloom in the north and peak bloom in Station 4. Station 6 was much further south than any of the others, far away from MIZ and the Polar Front. As the bloom does not usually start until June due to much later thermal stratification (Wassmann et al., 1999), it is likely that this station was only at the pre-bloom stage, usually dominated by naked flagellates (Wassmann et al., 1999), which explains the abundance of Phaeocystis pouchetii and other flagellates in this southern station. This was supported by the high nutrient content throughout the watercolumn.

4.2.3. Concentration of TEP across the study area

In this work the estimated TEP concentrations were approximately 80 mg L^{-1}. TEP are considered important in the regulation of stickiness of phytoplankton cells (Bar-Zeev et al., 2012; Thornton, 2002). Their total amount and characteristics vary between species and growth phases (Passow 2002a). Diatoms and Phaeocystis pouchetii blooms for example can produce large amounts of TEP (Passow & Alldredge, 1994). The concentrations in this work were orders of magnitude above other values (e.g. Meng et al., 2020; Passow, 2002b). For instance, in Fram Strait the highest concentration was around 500 µg L^{-1} with an average of less than 80 µg L^{-1} (Engel et al., 2017). Culture studies reported similar values to the data here (Meng et al., 2020), and one field study from the Adriatic Sea (11 mg L^{-1} Passow, 2002b) reported also substantially higher values. It cannot be excluded that dye deterioration in my study could have caused an overestimation of the TEP concentrations in sample vials that were stored for longer periods (Meng et al., 2020) as there was considerable time (17 weeks) between stain calibration and actual measurements in this study. However, the exceptionally high encountered Chl a concentrations may, at least partially, explain high TEP values recorded here. The wide range of applied methods for determining TEP (Meng et al., 2020; Passow, 2002b) can also cause varying results. Therefore, results shown in this study are not comparable to other studies and should be considered to demonstrate differences between stations, but not absolute values.

Interestingly, the measured concentrations of TEP followed the pattern in abundances of phytoplankton and specifically Chaetoceros spp. and Phaeocystis pouchetii abundances at Stations 4 and 6 (Figure 9). This is likely explained by the dominance of the two abovementioned algae at these stations. The general algal cells in stationary or nutrient limited phase produce higher amounts of TEP under deteriorating environmental conditions (Passow, 2002a). However high TEP production has also been observed during exponential algal growth (Penna et al., 1999). During exponential and stationary phases, the excretion of TEP happens both actively and passively (by permeation) (Passow, 2002a). While Station 1 TEP production can be linked to the strongest nutrient limitation, Stations 2 and 3 had increasing abundances of TEP-producing P. pouchetii. However, the high concentrations of TEP at Station 6 were surprising as the station was likely still in the pre-bloom stage and no nutrient limitation was

detected. Perhaps they can produce high amounts of TEP outside nutrient limitation (Penna et al., 1999).

4.2.4. NP adhesion experiment in Arctic protist communities

The experimental results demonstrate strong differences in the NP adherence to protist cells across species. All taxa except heterotrophic dinoflagellates had NPs adhered after the exposure. We had initially hypothesized that TEP producing taxa such as Chaetoceros and Phaeocystis would have the highest levels of adhered NPs because of their related stickiness. Surprisingly, this was not the case. Instead, the taxa with the highest numbers of adhered NPs relative to their abundance was Thalassiosira spp., and both mixo- and heterotrophic ciliates, which are not known as strong TEP producers. High TEP measurements in bulk samples were not necessarily related to high attachment rates for all species as these bulk measurements do not provide information on the species level. Adherence in different protist groups was relatively similar between stations, with the largest within-species difference in P. pouchetii. Interestingly, Phaeocystis both adherence and abundance followed the concentration of TEP for the most part. This makes it difficult to find the true relationships between these factors (abundance, adherence and TEP) as they covaried. In fact, protist abundance and the adherence of NPs followed each relatively well in all centric diatoms, mixotrophic ciliates and phototrophic flagellates, although statistical tests were not able to confirm this. The astonishingly high rate of adherence in the samples in relation to its abundance was found for mixotrophic ciliates, followed up by heterotrophic ciliates and Thalassiosira spp., driven by high NP adherence per cell. Compared to low contributions from the vastly more abundant TEP producers Chaetoceros and Phaeocystis, this indicates that other cell features appear to be of high importance. The effect of colonies in colony-forming diatoms was evident, as the minority of adherence occurred in single cells. The opposite was true for Phaeocystis, which however mainly occurred as single cells in the water samples. Interestingly, higher adherence was recorded for photo/mixotrophic groups rather than their heterotrophic counterparts.

These findings are surprising, considering that hetero-aggregation (NP-microalgal aggregate) with phytoplankton (for example Chaetoceros neogracile) had been observed and linked to the production of TEP/EPS (Bellingeri et al., 2020; Long et al., 2017; Mao et al., 2018). Perhaps

this means that contradictory to previous studies, the small, highly mucous and sticky colony-forming taxa avoid adherence better than larger and little TEP producing species. Presence of TEP does not automatically mean that aggregation of gel-like particles happens (Thornton, 2002), which, consecutively, could also be true to aggregation of NPs. Stickiness of TEP has been proven to be negatively correlated with algal abundance, and as healthy cells might exudate particles which counteract the production of TEP (Engel, 2000), cells can avoid coagulation (Kiørboe & Hansen, 1993).

The data suggests that other physiological factors may be more important for defining at which rate adherence occurs. Both Thalassiosira and Chaetoceros similarly have spines sticking out of their theca, but they differ in the material, shape, size, number and direction (organic threads from fultoportulae and setae, respectively). Thalassiosira are also covered in mucilage, but to a lesser extent than Chaetoceros and Phaeocystis. Chaetoceros create secondary colonies with elongated setae, which are connected. The distance between cells in chains are also much smaller than in Thalassiosira. Many of the NPs adhered to both of these diatom groups adhered to either the corner of the broad gridle view or between the cell chain (Figure 4). The main obvious difference in addition to the production of TEP is the cell size, Thalassiosira being twice the size of Chaetoceros recorded in this work. However, of the two only Thalassiosira have fultoportula processes, and in a study by Bellingeri et al. (2020) particles adhered to these structures in S. marinoi, which could explain the results. Since TEP was highly present throughout the stations and as the TEP matrix could not be seen in the fluorescent microscope, there might have been an underestimation for recorded adherence to Chaetoceros and Phaeocystis, as only particles connected to the cells or their visible external features were recorded as adherence. However, for Phaeocystis, mostly the non-motile gelatinous colonies are embedded in gel and the related error would be small. Ciliates are usually large (approximately 100 µm), as was observed in this study. They have cilia around the cytosome, and some may have specific housing for shelter, which both could contribute to adherence. For other protists, such as flagellates and dinoflagellates, their smooth surface and for dinoflagellates their polysaccharide shells probably provide little material for adherence as adherence rates were low. Ciliates can ingest some particles during the experiment as seen in this study and by for example Christaki et al., (1998). Having no separate categories for adhered and ingested particles likely led to an overestimation of adherence in these both ciliate groups. Regardless, this data still proves the astonishing level of interaction with NPs and ciliates. Conclusively it is clear from these results that neither abundance nor TEP can be considered

strong indicators for NP adherence patterns in mixed natural communities. In this context it is important to remember that this study captured late spring communities and different effects can be expected for the other seasons of the year, which differ in their algal composition (Rat'kova & Wassmann, 2002; Sergeeva et al., 2018).

The chosen treatment time was only 3 h here. However, based on results from previous studies (González-Fernández et al., 2019; Long et al., 2017; Sakhon et al., 2019), it may be that over a long-term exposure to NPs, TEP-producing phytoplankton could decrease interaction with NPs by higher excretion of TEP. As a result, it could be that NPs would adhere to this polysaccharide matrix with a subsequent physical boundary between the cells and the plastic particles effectively removing NPs from algal surfaces into TEP aggregates. This would not remove NPs altogether and some adherence would still occur to non-TEP producing taxa.

4.2.5. Other relevant studies to NP adhered protists

Nearly all studies about the interaction and toxic effects of MPs or NPs to phytoplankton have chosen microalgal monocultures with very high concentrations of added particles above typical naturally observed values, as introduced earlier (see Section 1.2.). While they give an indication to possible scenarios in areas with high levels of plastic pollution, it is important to incorporate environmentally relevant concentrations into these studies, as well as mixed community tests as done in this study. Regardless, they are useful to demonstrate potential effects of microalgal exposure to particles. Such species specific effects could be related to species specific adherence rates as observed in this study. González-Fernández et al. (2019) suggested that algal cells in the exponential growth phase and high energy requirements are particularly vulnerable to NPs, while in the stationary phase the aggregation of NPs may counteract the contact and toxicity effects of the particles. Species which produce TEP may counteract these effects in the stationary phase by homo- and hetero-aggregation (Mao et al., 2018). A study of Chlorella pyrenoidosa on NP exposure showed that cells exposed to a continuous concentration of NPs recovered from adverse effects, whereas accumulative concentration of particles prohibited the recovery of these effects and they became irreversible (Yang et al., 2021). Such effects could not be observed in this work as this short-term experiment included a single particle addition. The MNPs concentrations in the world's oceans are increasing and constantly replenished.

Thus, if algae are exposed to high, accumulative concentrations of particles over a long time, this may be more detrimental to phytoplankton communities than studies with continuous concentrations have previously showed. Responses to exposure differ for taxa. For example, in colony-forming diatoms, shortened chain-length is possible when interacting with NPs (Bellingeri et al., 2020), which may lead to changes in buoyancy. For heterotrophs, feeding on particles is an additional risk for exposure as we observed for the ciliates. Depending on for example the feeding strategy, some heterotrophic dinoflagellates may ingest MPs, which consecutively results in some of the abovementioned effects (Fulfer & Menden-Deuer, 2021; Su et al., 2020). Although there was no interaction between heterotrophic dinoflagellates and NPs in this study, there is still potential for interaction and ingestion if exposed for longer time (Fulfer & Menden-Deuer, 2021). Differing particle sizes might not result in different levels of ingestion for ciliates, as they are likely not able to distinguish prey from NPs (Y. Zhang et al., 2021), although even preferential selection of MPs over prey has been recorded (Bermúdez et al., 2021). Conclusively, a wide range of responses of phytoplankton to MNPs exposure has been demonstrated in single species experiments at beyond environmental concentrations which limits their value for field conditions. However, they should not be rejected as possible scenarios with increasing plastic pollution levels, and further investigations are needed.

The three highest adhering taxa relative to their abundance (Thalassiosira spp. and ciliates) could be subject to adverse effects under chronic exposure of NPs in the environment. For Thalassiosira sp., PVC MPs have shown temporary inhibitory rates of F_v/F_m, decreased Chl a content and lower cell density upon exposure (S. Wang et al., 2020). However, for T. weissiflogii, polyethylene did not inhibit growth beyond 10 h (Baudrimont et al., 2020). T. pseudonana protein-to-carbohydrate (P/C) ratio differed upon exposure to polystyrene, which makes TEP stickier (Shiu et al., 2020). T. pseudonana had higher growth inhibition, higher ROS and cell death with cell surface damage in 1.0 µm PS, whereas light shading, changes in gene expression and cellular pigments declined more strongly with 0.1 µm particles which could be due to higher adherence rates (B. Zhang et al., 2022). These studies show a wide variety of results, which could be a result from different polymer types, concentrations and even species differences. Thalassiosira spp. are very important to the diet of the copepod Calanus glacialis for their high fatty acid content (Søreide et al., 2010), and a major contributor to sympagic and phytoplankton blooms (Kvernvik et al., 2020), which means that any possible adverse effects in an interaction with NPs may prove harmful in these systems. For ciliates, abundance, body size and biomass has shown to decrease when they were exposed to PS no

matter the particle size (0.5 to 5 µm) (Y. Zhang et al., 2021). Significant ingestion has been observed (Bermúdez et al., 2021; Christaki et al., 1998; Y. Zhang et al., 2021), in addition to mitochondrial permeability, ROS and growth inhibition (Wu et al., 2021). Ciliates are microzooplankton which are grazed by mesozooplankton (Calbet & Saiz, 2005) and are thus important ecologically in connecting primary production to higher trophic levels (Fulfer & Menden-Deuer, 2021). Hence, if ciliates in the Polar Front undergo these effects from the previous studies, it may have consequences for higher trophic levels in this highly productive area.

1.2.3. Implications of species-specific NP adherence to the Polar Front

The polar Front is a highly productive area in the Barents Sea of high ecological and commercial value (Sakshaug, 1991), and as such, may be particularly vulnerable to marine pollutants. Primary production in the Polar Front varies annually (Reigstad et al., 2011) and some years production rates are exceptionally high (Børsheim & Drinkwater, 2014). The ecological implications of species-specific adherence may already become substantial if the three most adhering groups have adverse effects for zooplankton diet and therefore higher trophic levels.

Even though low adherence levels were observed in Chaetoceros in this work, the possibility of NPs embedded in cells, colonies and especially hetero- and homo-aggregates could act as a vertical sink of particles to the sea floor (C.-S. Chen et al., 2021) if microgel aggregates trap marine pollutants, which may affect their bioavailability (Shiu & Lee, 2017). Aggregation and incorporation of MNPs into marine snow could affect the sinking velocity of carbon to sediments (Walker et al., 2016), depending on the relative density of the polymer type (Casabianca et al., 2021). Larger aggregates have been observed in the presence of NPs (Shiu et al., 2020). If plastic particles in the water column get incorporated in marine snow via aggregation with TEP/EPS, it may turn these particles into the size ranges of ingestion for fish and other organisms (Thornton, 2002). Also the mass sinking of algae at the end of a bloom (Sakshaug, 1991) may transport adhered particles to the seafloor, away from the surface and consumption of herbivores. Herbivorous zooplankton graze on phytoplankton during blooms (Hansen et al., 1990; Tande & Båmstedt, 1985) transferring MNPs from phytoplankton to

zooplankton via grazing and even by direct ingestion (Cole et al., 2013). This may pose a risk to highly important and productive fish in the area, such as capelin (Gjøsæter, 1998) which feed on small zooplankton (Basedow et al., 2014). Such trophic transfer of NPs has been recorded throughout a system all the way from microalgae to fish in both freshwater (Chae et al., 2018) and marine systems (Kim et al., 2022) by adhesion to microalgal cells with adverse effects in fish, such as disturbances in liver tissue, lipid metabolism, embryos and gut permeability. Still, while biomagnification of plastic particles may still be uncertain, the existing additives and/or ab/adsorpted chemicals may get released into tissues in organisms, which may accumulate also in Arctic food webs (Diepens & Koelmans, 2018). Concentrations in exposure studies have been high and the risk of detected effects in natural populations should be evaluated with caution. Regardless, MNPs slowly accumulate in the ecosystems and such chronic exposure to particles even at lower concentrations may lead to build-up throughout the higher trophic levels (Chae et al., 2018), which may lead to direct or indirect harm to the organisms (Bergmann et al., 2022).

An additional feature of the Polar Front is the MIZ and its possible impact on MNP bioavailability. Sea ice is known to scavenge plastic and non-plastic particles from the surrounding waters as it forms (Obbard et al., 2014). This concentrates particles in the sea ice, and when the ice melts, it releases these particles back into the water column. However, possible hetero-aggregation of plastics with sticky EPS from sea ice algae as well as cryogenic gypsum of Phaeocystis blooms may enhance sinking to the seafloor (Bergmann et al., 2022; Hoffmann et al., 2020). Sea ice also traps airborne plastics (Bergmann et al., 2022). Therefore, sea ice additions to the available pool of particles is an important process to consider in the future. As mentioned earlier, the presence of plastics in the Arctic has already been confirmed at high levels (Tošić et al., 2020) and the import increases annually (Bergmann et al., 2022). Therefore, the risks for biota are rising across the Arctic and Barents Sea Polar Front and a combination of field and experimental studies should focus on the presence and ecological relevance of MNPs over complete seasonal cycles.

1.2.4. Methodological considerations

As for all studies, methodological restraints should be considered for evaluation of the reliability of data and to improve future studies. First, the treatment setup for the short-term field experiment did not include continuous mixing, reducing the encounter rate of NPs with cells, and potentially leading to an underestimations of cell specific adherence. Small differences in the density of the particles (1.055 g L^{-1}) and algae (Walsby & Xypolyta, 1977) might have caused separation during the experiment, reducing encounter rates. This could be avoided using for example a roller table which continuously mixes algae at an appropriate speed. Unfortunately, this setup was not available for the cruise. Furthermore, the observed NP concentration in the experimental bottles at the end of the exposure time was less than half of the target concentration: desired NPs concentration was 10 000 NPs mL^{-1}, whereas the measured concentration was 4800 ± 1400 NPs mL^{-1}. Several factors could be responsible for this. There might have been some errors in the dilution steps from the stock solution to the final treatment solution (one dilution step). While most studies using nanoparticles ensure particles are readily available and no aggregates are present through sonication (for example: Cole et al., 2013), the stock solution in this study was mixed vigorously by hand for approximately 15 seconds. Adherence of the plastic particles to the various containers used in the study could be leading to abundance reductions. It is suggested to test the final concentrations of NPs prior to the experiment in each treatment flask for further calculations.

Adherence of particles in this study was measured visually using a fluorescence microscope, which poses challenges of its own. Visual inspections made with this method may not be precise enough to confirm or reject true adherence of particles to protist cells in all cases. Microalgae and NPs may have surfaced on top of each other during the filtration process without any actual interaction between particle and cell. Additionally, the smallest DAPI stained cells were hard to see identify due to the fading dye, which might have led to an underestimation in especially heterotrophic flagellates. A study on the less abundant non-diatom taxa should use larger filtration volumes or scan larger filter areas which was not possible considering the limited time available for this thesis. The low estimates for colony sizes, especially in Phaeocystis spp. could have two causes. First, the low number of views analyzed per filter meant that the encounter of Phaeocystis colonies was low. Secondly, formaldehyde may sometimes destroy EPS and TEP matrixes, which may have resulted in breaking up of these colonies during fixing, staining and filtering the samples (Salama et al., 2016). For a more accurate estimation for true adherence, a Scanning Electron Microscope (SEM) would yield higher resolution images to show the spatial variations and structure of

cells and adherence. This would possibly increase the taxonomic resolution of data also, as some groups of protists were not recorded at all stations.

Another consideration is the length of the exposure time chosen here, which was short (3 hours), when most existing studies of microalgal exposure to NPs or MPs chose durations of several days. Here, only adherence of particles to cells was studied, in addition to measuring in situ TEP concentrations in the vicinity of the Polar Front. Using longer exposure times (as originally planned for the culture experiment) combined with a boarder range of test variables would give an indication for possible physiological effects from the NP-algae interaction (24+ h).

2. Conclusion and outlook

This study provided a unique insight into the initial adherence of nanoplastics in natural Arctic protist communities. This work was in contrast to the vast majority of experimental studies exposing monocultures with extremely high micro- and nanoplastic concentrations, with some beyond realistic natural concentrations. Although micro- and nanoplastic field research still needs major improvements in methodology, this study provided insights for species-specific adherence, which may not necessarily be driven by the stickiness of TEP in the community, but rather other physical features of the protists. While no a strong relationship between TEP and adherence was found, it is possible that the potential for TEP to adhere particles may increase towards the end of a diatom and Phaeocystis bloom, as older TEP modified by bacteria is stickier than fresh transparent particles from microalgae (Rochelle-Newall et al., 2010).

The species-specific data indicate the potential for a seasonal cycle in the attachment of NPs driven by the seasonality of phytoplankton and protist communities. As diatom and Phaeocystis dominance ends towards the end of the bloom and are replaced by flagellates (Rat'kova & Wassmann, 2002; Verity et al., 2002), the level of adherence of NPs in the community overall decreases. Due to very low biomass of the winter phytoplankton community, the attachment is also minimal. While only being a snapshot of the spring bloom and the composition of the phytoplankton community in the Polar Front area, general patterns of species and community level NP adherence could be demonstrated in this work. These results should be considered as indication of selectivity, highlighting the species-specific adherence of particles, and thus possibly leading to a seasonal cycle of attachment, as mentioned above.

For future studies it is recommended to shift the focus of experiments on more complex community levels instead of single species. Testing other biochemical responses, such as changes in TEP production throughout the exposure time, Chl *a*, F_v/F_m and ROS over a longer exposure would yield more in-depth information about the possible effects of algae at the community level. As highlighted in Sections 1.2. and 4.2.5., the adverse effects of exposure to NPs are highly variable and depend on the phases of the algae, concentration, size and physical features of the particles. To study whether these effects are realistic to the Polar Front or Barents Sea area, it is of utmost importance for future studies to use natural communities from

the area of interest, and perform long-term exposures with several types of particles, as clean virgin NPs are not representative of the particle composition observed in the oceans. Standardized methods for testing relevant concentrations, polymer sizes and types on top of exposure length are strongly urged to be able to implement these findings into management of such valuable areas. Finally, we suggest studies which focus on a) full seasonal cycle study of NP presence and adherence in highly productive areas, and b) chronic physiological effects on natural communities, to fill the massive knowledge gaps which still exist in natural phytoplankton communities around the world.

3. References

Andrady, A. (2015). Persistence of plastic litter in the oceans. In *Marine anthropogenic litter* (pp. 57–72). Springer.

Arar, E. J., & Collins, G. B. (1997). *Method 445.o: In vitro Determination of Chlorophyll a and Phaeophytin a in Marine and Freshwater Algae Fluorescence*.

Arruda Fatibello, S. H. S., Henriques Vieira, A. A., & Fatibello-Filho, O. (2004). A rapid spectrophotometric method for the determination of transparent exopolymer particles (TEP) in freshwater. *Talanta*, *62*(1), 81–85. https://doi.org/10.1016/S0039-9140(03)00417-X

Ayres, S. L. (2017). *Cell Density (Mass per unit Volume) of Diatom Cells and Chains in relation to their Size, Growth, and Nutritional Condition* [The University of Maine]. https://digitalcommons.library.umaine.edu/etd/2678

Bar-Zeev, E., Berman-Frank, I., Girshevitz, O., & Berman, T. (2012). Revised paradigm of aquatic biofilm formation facilitated by microgel transparent exopolymer particles. *Proceedings of the National Academy of Sciences*, *109*(23), 9119–9124. https://doi.org/10.1073/pnas.1203708109

Basedow, S. L., Zhou, M., & Tande, K. S. (2014). Secondary production at the Polar Front, Barents Sea, August 2007. *Journal of Marine Systems*, *130*, 147–159. https://doi.org/10.1016/j.jmarsys.2013.07.015

Baudrimont, M., Arini, A., Guégan, C., Venel, Z., Gigault, J., Pedrono, B., Prunier, J., Maurice, L., Ter Halle, A., & Feurtet-Mazel, A. (2020). Ecotoxicity of polyethylene nanoplastics from the North Atlantic oceanic gyre on freshwater and marine organisms

(microalgae and filter-feeding bivalves). *Environmental Science and Pollution Research*, *27*(4), 3746–3755. https://doi.org/10.1007/s11356-019-04668-3

Bellingeri, A., Casabianca, S., Capellacci, S., Faleri, C., Paccagnini, E., Lupetti, P., Koelmans, A. A., Penna, A., & Corsi, I. (2020). Impact of polystyrene nanoparticles on marine diatom Skeletonema marinoi chain assemblages and consequences on their ecological role in marine ecosystems. *Environmental Pollution*, *262*, 114268. https://doi.org/10.1016/j.envpol.2020.114268

Bergmann, M., Collard, F., Fabres, J., Gabrielsen, G. W., Provencher, J. F., Rochman, C. M., van Sebille, E., & Tekman, M. B. (2022). Plastic pollution in the Arctic. *Nature Reviews Earth & Environment*, 1–15. https://doi.org/10.1038/s43017-022-00279-8

Bermúdez, J. R., Metian, M., Oberhänsli, F., Taylor, A., & Swarzenski, P. W. (2021). Preferential grazing and repackaging of small polyethylene microplastic particles (≤ 5 µm) by the ciliate Sterkiella sp. *Marine Environmental Research*, *166*, 105260. https://doi.org/10.1016/j.marenvres.2021.105260

Bogstad, B., Gjøsæter, H., Haug, T., & Lindstrøm, U. (2015). A review of the battle for food in the Barents Sea: Cod vs. marine mammals. *Frontiers in Ecology and Evolution*, *3*. https://www.frontiersin.org/articles/10.3389/fevo.2015.00029

Børsheim, K. Y., & Drinkwater, K. F. (2014). Different temperature adaptation in Arctic and Atlantic heterotrophic bacteria in the Barents Sea Polar Front region. *Journal of Marine Systems*, *130*, 160–166. https://doi.org/10.1016/j.jmarsys.2012.09.007

Børsheim, K. Y., Milutinović, S., & Drinkwater, K. F. (2014). TOC and satellite-sensed chlorophyll and primary production at the Arctic Front in the Nordic Seas. *Journal of Marine Systems*, *139*, 373–382. https://doi.org/10.1016/j.jmarsys.2014.07.012

Botterell, Z. L. R., Bergmann, M., Hildebrandt, N., Krumpen, T., Steinke, M., Thompson, R. C., & Lindeque, P. K. (2022). Microplastic ingestion in zooplankton from the Fram Strait in the Arctic. *Science of The Total Environment*, *831*, 154886. https://doi.org/10.1016/j.scitotenv.2022.154886

Calbet, A., & Saiz, E. (2005). The ciliate-copepod link in marine ecosystems. *Aquatic Microbial Ecology*, *38*(2), 157–167. https://doi.org/10.3354/ame038157

Casabianca, S., Bellingeri, A., Capellacci, S., Sbrana, A., Russo, T., Corsi, I., & Penna, A. (2021). Ecological implications beyond the ecotoxicity of plastic debris on marine phytoplankton assemblage structure and functioning. *Environmental Pollution*, *290*, 118101. https://doi.org/10.1016/j.envpol.2021.118101

Chae, Y., Kim, D., Kim, S. W., & An, Y.-J. (2018). Trophic transfer and individual impact of nano-sized polystyrene in a four-species freshwater food chain. *Scientific Reports*, *8*(1), Article 1. https://doi.org/10.1038/s41598-017-18849-y

Chamnansinp, A., Li, Y., Lundholm, N., & Moestrup, Ø. (2013). Global diversity of two widespread, colony-forming diatoms of the marine plankton, Chaetoceros socialis (syn. C. radians) and Chaetoceros gelidus sp. Nov. *Journal of Phycology*, *49*(6), 1128–1141. https://doi.org/10.1111/jpy.12121

Chen, C.-S., Shiu, R.-F., Hsieh, Y.-Y., Xu, C., Vazquez, C. I., Cui, Y., Hsu, I. C., Quigg, A., Santschi, P. H., & Chin, W.-C. (2021). Stickiness of extracellular polymeric substances on different surfaces via magnetic tweezers. *Science of The Total Environment*, *757*, 143766. https://doi.org/10.1016/j.scitotenv.2020.143766

Chen, Y., Ling, Y., Li, X., Hu, J., Cao, C., & He, D. (2020). Size-dependent cellular internalization and effects of polystyrene microplastics in microalgae P. helgolandica

var. Tsingtaoensis and S. quadricauda. *Journal of Hazardous Materials*, *399*, 123092. https://doi.org/10.1016/j.jhazmat.2020.123092

Christaki, U., Dolan, J. R., Pelegri, S., & Rassoulzadegan, F. (1998). Consumption of picoplankton-size particles by marine ciliates: Effects of physiological state of the ciliate and particle quality. *Limnology and Oceanography*, *43*(3), 458–464. https://doi.org/10.4319/lo.1998.43.3.0458

Cole, M., Lindeque, P., Fileman, E., Halsband, C., Goodhead, R., Moger, J., & Galloway, T. S. (2013). Microplastic Ingestion by Zooplankton. *Environmental Science & Technology*, *47*(12), 6646–6655. https://doi.org/10.1021/es400663f

Collard, F., & Ask, A. (2021). Plastic ingestion by Arctic fauna: A review. *Science of The Total Environment*, *786*, 147462. https://doi.org/10.1016/j.scitotenv.2021.147462

Cózar, A., Martí, E., Duarte, C. M., García-de-Lomas, J., van Sebille, E., Ballatore, T. J., Eguíluz, V. M., González-Gordillo, J. I., Pedrotti, M. L., Echevarría, F., Troublè, R., & Irigoien, X. (2017). The Arctic Ocean as a dead end for floating plastics in the North Atlantic branch of the Thermohaline Circulation. *Science Advances*, *3*(4), e1600582. https://doi.org/10.1126/sciadv.1600582

Diepens, N. J., & Koelmans, A. A. (2018). Accumulation of Plastic Debris and Associated Contaminants in Aquatic Food Webs. *Environmental Science & Technology*, *52*(15), 8510–8520. https://doi.org/10.1021/acs.est.8b02515

Elgarahy, A. M., Akhdhar, A., & Elwakeel, K. Z. (2021). Microplastics prevalence, interactions, and remediation in the aquatic environment: A critical review. *Journal of Environmental Chemical Engineering*, *9*(5), 106224. https://doi.org/10.1016/j.jece.2021.106224

Engel, A. (2000). The role of transparent exopolymer particles (TEP) in the increase in apparent particle stickiness (α) during the decline of a diatom bloom. *Journal of Plankton Research*, *22*(3), 485–497. https://doi.org/10.1093/plankt/22.3.485

Engel, A., Piontek, J., Metfies, K., Endres, S., Sprong, P., Peeken, I., Gäbler-Schwarz, S., & Nöthig, E.-M. (2017). Inter-annual variability of transparent exopolymer particles in the Arctic Ocean reveals high sensitivity to ecosystem changes. *Scientific Reports*, *7*(1), Article 1. https://doi.org/10.1038/s41598-017-04106-9

Falk-Petersen, S., Mayzaud, P., Kattner, G., & Sargent, J. R. (2009). Lipids and life strategy of Arctic Calanus. *Marine Biology Research*, *5*(1), 18–39. https://doi.org/10.1080/17451000802512267

Fulfer, V. M., & Menden-Deuer, S. (2021). Heterotrophic Dinoflagellate Growth and Grazing Rates Reduced by Microplastic Ingestion. *Frontiers in Marine Science*, *8*. https://www.frontiersin.org/articles/10.3389/fmars.2021.716349

Gawarkiewicz, G., & Plueddemann, A. J. (1995). Topographic control of thermohaline frontal structure in the Barents Sea Polar Front on the south flank of Spitsbergen Bank. *Journal of Geophysical Research: Oceans*, *100*(C3), 4509–4524. https://doi.org/10.1029/94JC02427

Geyer, R., Jambeck, J. R., & Law, K. L. (2017). Production, use, and fate of all plastics ever made. *Science Advances*, *3*(7), e1700782. https://doi.org/10.1126/sciadv.1700782

Gjøsæter, H. (1995). Pelagic Fish and the Ecological Impact of the Modern Fishing Industry in the Barents Sea. *Arctic*, *48*(3), 267–278.

Gjøsæter, H. (1998). The population biology and exploitation of capelin (Mallotus villosus) in the barents sea. *Sarsia*, *83*(6), 453–496. https://doi.org/10.1080/00364827.1998.10420445

González-Fernández, C., Toullec, J., Lambert, C., Le Goïc, N., Seoane, M., Moriceau, B., Huvet, A., Berchel, M., Vincent, D., Courcot, L., Soudant, P., & Paul-Pont, I. (2019). Do transparent exopolymeric particles (TEP) affect the toxicity of nanoplastics on Chaetoceros neogracile? *Environmental Pollution*, *250*, 873–882. https://doi.org/10.1016/j.envpol.2019.04.093

Grønted, J., & Seidenfaden, G. (1938). The Godthaab expedition 1928. *CA Reitzel*, *82(5)*, 1–136.

Halse, G. R., & Syvertsen, E. E. (1996). Chapter 2—Marine Diatoms. In C. R. Tomas (Ed.), *Identifying Marine Diatoms and Dinoflagellates* (pp. 5–385). Academic Press. https://doi.org/10.1016/B978-012693015-3/50005-X

Hansen, B., Berggreen, U. C., Tande, K. S., & Eilertsen, H. C. (1990). Post-bloom grazing byCalanus glacialis, C. finmarchicus andC. hyperboreus in the region of the Polar Front, Barents Sea. *Marine Biology*, *104*(1), 5–14. https://doi.org/10.1007/BF01313151

Hansen, E., & Eilertsen, H. Chr. (2007). Do the polyunsaturated aldehydes produced by Phaeocystis pouchetii (Hariot) Lagerheim influence diatom growth during the spring bloom in Northern Norway? *Journal of Plankton Research*, *29*(1), 87–96. https://doi.org/10.1093/plankt/fbl065

Harrison, W. G., & Cota, G. F. (1991). Primary production in polar waters: Relation to nutrient availability. *Polar Research*, *10*(1), 87–104. https://doi.org/10.3402/polar.v10i1.6730

Hoffmann, L., Eggers, S. L., Allhusen, E., Katlein, C., & Peeken, I. (2020). Interactions between the ice algae Fragillariopsis cylindrus and microplastics in sea ice. *Environment International*, *139*, 105697. https://doi.org/10.1016/j.envint.2020.105697

Kanhai, L. D. K., Gardfeldt, K., Krumpen, T., Thompson, R. C., & O'Connor, I. (2020). Microplastics in sea ice and seawater beneath ice floes from the Arctic Ocean. *Scientific Reports*, *10*(1), Article 1. https://doi.org/10.1038/s41598-020-61948-6

Kim, L., Cui, R., Il Kwak, J., & An, Y.-J. (2022). Trophic transfer of nanoplastics through a microalgae–crustacean–small yellow croaker food chain: Inhibition of digestive enzyme activity in fish. *Journal of Hazardous Materials*, *440*, 129715. https://doi.org/10.1016/j.jhazmat.2022.129715

Kiørboe, T., & Hansen, J. L. S. (1993). Phytoplankton aggregate formation: Observations of patterns and mechanisms of cell sticking and the significance of exopolymeric material. *Journal of Plankton Research*, *15*(9), 993–1018. https://doi.org/10.1093/plankt/15.9.993

Knutsen, H., Cyvin, J. B., Totland, C., Lilleeng, Ø., Wade, E. J., Castro, V., Pettersen, A., Laugesen, J., Møskeland, T., & Arp, H. P. H. (2020). Microplastic accumulation by tube-dwelling, suspension feeding polychaetes from the sediment surface: A case study from the Norwegian Continental Shelf. *Marine Environmental Research*, *161*, 105073. https://doi.org/10.1016/j.marenvres.2020.105073

Kögel, T., Hamilton, B. M., Granberg, M. E., Provencher, J., Hammer, S., Gomiero, A., Magnusson, K., & Lusher, A. L. (2022). Current efforts on microplastic monitoring in Arctic fish and how to proceed. *Arctic Science*. https://doi.org/10.1139/as-2021-0057

Krause, J. W., Duarte, C. M., Marquez, I. A., Assmy, P., Fernández-Méndez, M., Wiedmann, I., Wassmann, P., Kristiansen, S., & Agustí, S. (2018). Biogenic silica production and diatom dynamics in the Svalbard region during spring. *Biogeosciences*, *15*(21), 6503–6517. https://doi.org/10.5194/bg-15-6503-2018

Kvernvik, A. C., Rokitta, S. D., Leu, E., Harms, L., Gabrielsen, T. M., Rost, B., & Hoppe, C. J. M. (2020). Higher sensitivity towards light stress and ocean acidification in an Arctic sea-ice-associated diatom compared to a pelagic diatom. *New Phytologist*, *226*(6), 1708–1724. https://doi.org/10.1111/nph.16501

Li, P., Li, Q., Hao, Z., Yu, S., & Liu, J. (2020). Analytical methods and environmental processes of nanoplastics. *Journal of Environmental Sciences*, *94*, 88–99. https://doi.org/10.1016/j.jes.2020.03.057

Long, M., Paul-Pont, I., Hégaret, H., Moriceau, B., Lambert, C., Huvet, A., & Soudant, P. (2017). Interactions between polystyrene microplastics and marine phytoplankton lead to species-specific hetero-aggregation. *Environmental Pollution*, *228*, 454–463. https://doi.org/10.1016/j.envpol.2017.05.047

Lynn, D. (2009). Ciliates. In M. Schaechter (Ed.), *Encyclopedia of Microbiology (Third Edition)* (pp. 578–592). Academic Press. https://doi.org/10.1016/B978-012373944-5.00248-0

Makarevich, P. R., Larionov, V. V., Vodopyanova, V. V., Bulavina, A. S., Ishkulova, T. G., Venger, M. P., Pastukhov, I. A., & Vashchenko, A. V. (2021). Phytoplankton of the Barents Sea at the Polar Front in Spring. *Oceanology*, *61*(6), 930–943. https://doi.org/10.1134/S0001437021060084

Mao, Y., Ai, H., Chen, Y., Zhang, Z., Zeng, P., Kang, L., Li, W., Gu, W., He, Q., & Li, H. (2018). Phytoplankton response to polystyrene microplastics: Perspective from an entire growth period. *Chemosphere*, *208*, 59–68. https://doi.org/10.1016/j.chemosphere.2018.05.170

Meng, S., Meng, X., Fan, W., Liang, D., Wang, L., Zhang, W., & Liu, Y. (2020). The role of transparent exopolymer particles (TEP) in membrane fouling: A critical review. *Water Research*, *181*, 115930. https://doi.org/10.1016/j.watres.2020.115930

Moore, R. C., Loseto, L., Noel, M., Etemadifar, A., Brewster, J. D., MacPhee, S., Bendell, L., & Ross, P. S. (2020). Microplastics in beluga whales (Delphinapterus leucas) from the Eastern Beaufort Sea. *Marine Pollution Bulletin*, *150*, 110723. https://doi.org/10.1016/j.marpolbul.2019.110723

Obbard, R. W., Sadri, S., Wong, Y. Q., Khitun, A. A., Baker, I., & Thompson, R. C. (2014). Global warming releases microplastic legacy frozen in Arctic Sea ice. *Earth's Future*, *2*(6), 315–320. https://doi.org/10.1002/2014EF000240

Passow, U. (2002a). Production of transparent exopolymer particles (TEP) by phyto- and bacterioplankton. *Marine Ecology Progress Series*, *236*, 1–12. https://doi.org/10.3354/meps236001

Passow, U. (2002b). Transparent exopolymer particles (TEP) in aquatic environments. *Progress in Oceanography*, *55*(3), 287–333. https://doi.org/10.1016/S0079-6611(02)00138-6

Passow, U., & Alldredge, A. L. (1994). Distribution, size and bacterial colonization of transparent exopolymer particles (TEP) in the ocean. *Marine Ecology Progress Series*, *113*(1/2), 185–198.

Penna, A., Berluti, S., & Magnani, M. (1999). Influence of nutrient ratios on the in vitro extracellular polysaccharide production by marine diatoms from the Adriatic Sea. *Journal of Plankton Research*, *21*(9), 1681–1690. https://doi.org/10.1093/plankt/21.9.1681

Pfirman, S., Bauch, D., & Gammelsrød, T. (1994). *The northern Barents Sea: Water mass distribution and modification* (O. M. Johannessen, R. D. Muench, & J. E. Overland, Eds.; pp. 77–94). AGU (American Geophysical Union). https://doi.org/10.1029/GM085p0077

Porter, K. G., & Feig, Y. S. (1980). The use of DAPI for identifying and counting aquatic microflora1. *Limnology and Oceanography*, *25*(5), 943–948. https://doi.org/10.4319/lo.1980.25.5.0943

Rai, P. K., Kumar, V., Sonne, C., Lee, S. S., Brown, R. J. C., & Kim, K.-H. (2021). Progress, prospects, and challenges in standardization of sampling and analysis of micro- and nano-plastics in the environment. *Journal of Cleaner Production*, *325*, 129321. https://doi.org/10.1016/j.jclepro.2021.129321

Rat'kova, T. N., & Wassmann, P. (2002). Seasonal variation and spatial distribution of phyto- and protozooplankton in the central Barents Sea. *Journal of Marine Systems*, *38*(1), 47–75. https://doi.org/10.1016/S0924-7963(02)00169-0

Reid Jr., J. L. (1962). On Circulation, Phosphate-Phosphorus Content, and Zooplankton Volumes in the Upper Part of the Pacific Ocean1. *Limnology and Oceanography*, *7*(3), 287–306. https://doi.org/10.4319/lo.1962.7.3.0287

Reigstad, M., Carroll, J., Slagstad, D., Ellingsen, I., & Wassmann, P. (2011). Intra-regional comparison of productivity, carbon flux and ecosystem composition within the northern Barents Sea. *Progress in Oceanography*, *90*(1), 33–46. https://doi.org/10.1016/j.pocean.2011.02.005

Rey, F., & Skjodal, H. R. (1987). Consumption of silicic acid below the euphotic zone by sendimenting diatom blooms in the Barents Sea. *Marine Ecology Progress Series*, *36*, 307–312.

Rochelle-Newall, E. J., Mari, X., & Pringault, O. (2010). Sticking properties of transparent exopolymeric particles (TEP) during aging and biodegradation. *Journal of Plankton Research*, *32*(10), 1433–1442. https://doi.org/10.1093/plankt/fbq060

Sakhon, E. G., Mukhanov, V. S., & Khanaychenko, A. N. (2019). Phytoplankton Exopolymers Enhance Adhesion of Microplastic Particles to Submersed Surfaces. *Ecologica Montenegrina*, *23*, 60–69. https://doi.org/10.37828/em.2019.23.8

Sakshaug, E. (1991). Food webs and primary production in the Barents Sea. *Polar Biology*, *4*, 1–8.

Salama, Y., Chennaoui, M., Sylla, A., Mountadar, M., Rihani, M., & Assobhei, O. (2016). Characterization, structure, and function of extracellular polymeric substances (EPS) of microbial biofilm in biological wastewater treatment systems: A review. *Desalination and Water Treatment*, *57*(35), 16220–16237. https://doi.org/10.1080/19443994.2015.1077739

Sebille, E. van, England, M. H., & Froyland, G. (2012). Origin, dynamics and evolution of ocean garbage patches from observed surface drifters. *Environmental Research Letters*, *7*(4), 044040. https://doi.org/10.1088/1748-9326/7/4/044040

Sergeeva, V. M., Zhitina, L. S., Mosharov, S. A., Nedospasov, A. A., & Polukhin, A. A. (2018). Phytoplankton Community Structure in the Polar Front of the Eastern Barents Sea at the End of the Growth Season | SpringerLink. *Oceanology*, *58*, 700–709.

Shiu, R.-F., & Lee, C.-L. (2017). Effects of anthropogenic surfactants on the conversion of marine dissolved organic carbon and microgels. *Marine Pollution Bulletin*, *117*(1), 156–160. https://doi.org/10.1016/j.marpolbul.2017.01.051

Shiu, R.-F., Vazquez, C. I., Chiang, C.-Y., Chiu, M.-H., Chen, C.-S., Ni, C.-W., Gong, G.-C., Quigg, A., Santschi, P. H., & Chin, W.-C. (2020). Nano- and microplastics trigger secretion of protein-rich extracellular polymeric substances from phytoplankton. *Science of The Total Environment*, *748*, 141469. https://doi.org/10.1016/j.scitotenv.2020.141469

Slagstad, D., & Støle-Hansen, K. (1991). Dynamics of plankton growth in the Barents Sea: Model studies. *Polar Research*, *10*(1), 173–186. https://doi.org/10.1111/j.1751-8369.1991.tb00643.x

Søreide, J. E., Leu, E., Berge, J., Graeve, M., & Falk-Petersen, S. (2010). Timing of blooms, algal food quality and Calanus glacialis reproduction and growth in a changing Arctic. *Global Change Biology*, *16*(11), 3154–3163. https://doi.org/10.1111/j.1365-2486.2010.02175.x

Steidinger, K. A., & Jangen, K. (1997). Chapter 3—Dinoflagellates. In C. R. Tomas (Ed.), *Identifying Marine Phytoplankton* (pp. 387–584). Academic Press. https://doi.org/10.1016/B978-012693018-4/50005-7

Su, Y., Zhang, K., Zhou, Z., Wang, J., Yang, X., Tang, J., Li, H., & Lin, S. (2020). Microplastic exposure represses the growth of endosymbiotic dinoflagellate Cladocopium goreaui in culture through affecting its apoptosis and metabolism. *Chemosphere*, *244*, 125485. https://doi.org/10.1016/j.chemosphere.2019.125485

Tande, K. S., & Båmstedt, U. (1985). Grazing rates of the copepods Calanus glacialis and C. finmarchicus in arctic waters of the Barents Sea. *Marine Biology*, *87*(3), 251–258. https://doi.org/10.1007/BF00397802

ter Halle, A., Ladirat, L., Gendre, X., Goudouneche, D., Pusineri, C., Routaboul, C., Tenailleau, C., Duployer, B., & Perez, E. (2016). Understanding the Fragmentation Pattern of Marine Plastic Debris. *Environmental Science & Technology*, *50*(11), 5668–5675. https://doi.org/10.1021/acs.est.6b00594

Thornton, D. C. O. (2002). Diatom aggregation in the sea: Mechanisms and ecological implications. *European Journal of Phycology*, *37*(2), 149–161. https://doi.org/10.1017/S0967026202003657

Throndsen, J. (1997). Chapter 5—The Planktonic Marine Flagellates. In C. R. Tomas (Ed.), *Identifying Marine Phytoplankton* (pp. 591–729). Academic Press. https://doi.org/10.1016/B978-012693018-4/50007-0

Tošić, T. N., Vruggink, M., & Vesman, A. (2020). Microplastics quantification in surface waters of the Barents, Kara and White Seas. *Marine Pollution Bulletin*, *161*, 111745. https://doi.org/10.1016/j.marpolbul.2020.111745

Turner, A., Arnold, R., & Williams, T. (2020). Weathering and persistence of plastic in the marine environment: Lessons from LEGO. *Environmental Pollution*, *262*, 114299. https://doi.org/10.1016/j.envpol.2020.114299

Verity, P. G., Wassmann, P., Frischer, M. E., Howard-Jones, M. H., & Allen, A. E. (2002). Grazing of phytoplankton by microzooplankton in the Barents Sea during early summer. *Journal of Marine Systems*, *38*(1), 109–123. https://doi.org/10.1016/S0924-7963(02)00172-0

von Quillfeldt, C. (1996). *Ice Algae and Phytoplankton in North Norwegian and Arctic Waters: Species Composition, Succession and Distribution* [Doctoral dissertation]. University of Tromsø.

von Quillfeldt, C. H. von. (2000). *Common Diatom Species in Arctic Spring Blooms: Their Distribution and Abundance*. *43*(6), 499–516. https://doi.org/10.1515/BOT.2000.050

Walker, B. D., Beaupré, S. R., Guilderson, T. P., McCarthy, M. D., & Druffel, E. R. M. (2016). Pacific carbon cycling constrained by organic matter size, age and composition relationships. *Nature Geoscience*, *9*(12), Article 12. https://doi.org/10.1038/ngeo2830

Walsby, A. E., & Xypolyta, A. (1977). The form resistance of chitan fibres attached to the cells of Thalassiosira fluviatilis Hustedt. *British Phycological Journal*, *12*(3), 215–223. https://doi.org/10.1080/00071617700650231

Wang, S., Wang, Y., Liang, Y., Cao, W., Sun, C., Ju, P., & Zheng, L. (2020). The interactions between microplastic polyvinyl chloride and marine diatoms: Physiological, morphological, and growth effects. *Ecotoxicology and Environmental Safety*, *203*, 111000. https://doi.org/10.1016/j.ecoenv.2020.111000

Wang, S.-C., Liu, F.-F., Huang, T.-Y., Fan, J.-L., Gao, Z.-Y., & Liu, G.-Z. (2021). Effects of Nanoplastics on the Dinoflagellate Amphidinium carterae Hulburt from the Perspectives of Algal Growth, Oxidative Stress and Hemolysin Production. *Nanomaterials*, *11*(10), Article 10. https://doi.org/10.3390/nano11102471

Wassmann, P., Ratkova, T., Andreassen, I., Vernet, M., Pedersen, G., & Rey, F. (1999). Spring Bloom Development in the Marginal Ice Zone and the Central Barents Sea. *Marine Ecology*, *20*(3–4), 321–346. https://doi.org/10.1046/j.1439-0485.1999.2034081.x

Wu, C., Guo, W.-B., Liu, Y.-Y., Yang, L., & Miao, A.-J. (2021). Perturbation of calcium homeostasis and multixenobiotic resistance by nanoplastics in the ciliate Tetrahymena thermophila. *Journal of Hazardous Materials*, *403*, 123923. https://doi.org/10.1016/j.jhazmat.2020.123923

Yang, W., Gao, P., Nie, Y., Huang, J., Wu, Y., Wan, L., Ding, H., & Zhang, W. (2021). Comparison of the effects of continuous and accumulative exposure to nanoplastics on microalga Chlorella pyrenoidosa during chronic toxicity. *Science of The Total Environment*, *788*, 147934. https://doi.org/10.1016/j.scitotenv.2021.147934

Zaki, M. R. M., & Aris, A. Z. (2022). An overview of the effects of nanoplastics on marine organisms. *Science of The Total Environment*, *831*, 154757. https://doi.org/10.1016/j.scitotenv.2022.154757

Zhang, B., Tang, X., Liu, Q., Li, L., Zhao, Y., & Zhao, Y. (2022). Different effecting mechanisms of two sized polystyrene microplastics on microalgal oxidative stress and photosynthetic responses. *Ecotoxicology and Environmental Safety*, *244*, 114072. https://doi.org/10.1016/j.ecoenv.2022.114072

Zhang, Y., Wang, J., Geng, X., & Jiang, Y. (2021). Does microplastic ingestion dramatically decrease the biomass of protozoa grazers? A case study on the marine ciliate Uronema marinum. *Chemosphere*, *267*, 129308. https://doi.org/10.1016/j.chemosphere.2020.129308

Appendix

Appendix A: Chemical composition of artificial sea water (ASW).

Compound name	g L^{-1}
Sodium chloride	24.53
Magnesium Chloride	5.20
Sodium sulfate	4.09
Calcium chloride	1.16
Potassium chloride	0.695
Sodium bicarbonate	0.201
Potassium bromide	0.101
Boric acid	0.027
Strontium chloride	0.025
Sodium fluoride	0.003
MilliQ	988.968
Total	1.025g L-1